Platelets supply p38 MAPK signaling that licenses pro-inflammatory cytokine responses of human monocytes

Ibrahim Hawwari[1], Nathalia Sofia Rosero Reyes[1], Lucas S. Ribeiro[1], Agnieszka Demczuk[1], Lino L Teichmann, Lisa Meffert, Damien Bertheloot[1], and Bernardo S. Franklin[1*]

1) Institute of Innate Immunity, University Hospitals, Medical Faculty, University of Bonn, Bonn, Germany
2) Department of Medicine III, University Hospital Bonn, Bonn, Germany.

*Correspondence: franklin@uni-bonn.de

KEYWORDS: Cytokines, Immunoparalysis, Immune Thrombocytopenia, Toll-like Receptors, Inflammasomes.

HIGHLIGHTS

- Platelets are essential to monocyte pro-inflammatory TLR and NLR responses.
- Platelet depletion causes a dynamic and reversible transcriptional reprogramming of human monocytes;
- Platelet supplementation reverts monocyte immunoparalysis in immune thrombocytopenia;
- Platelets supply p38 MAPK signalling that licenses full cytokine responses of human monocytes.

ABSTRACT

Classical CD14$^+$ monocytes are the predominant monocyte population in human blood. They are primarily engaged in host defense programs and secrete pro-inflammatory cytokines that orchestrate immune responses. While aberrant monocyte activity elicits cytokine storms, dysfunctional monocytes are associated with immunoparalysis, an equally life-threatening state of immunosuppression observed in severe sepsis, trauma, or respiratory viral infections. Hence, unraveling the mechanisms controlling monocyte functions is paramount in diverse clinical settings. Here, we reveal a critical dependency on platelets for the pro-inflammatory cytokine responses of human monocytes. We found that platelet removal from freshly isolated primary human monocytes causes monocyte immunoparalysis, characterized by transcriptional shut down of pro-inflammatory genes, and impaired cytokine secretion upon Toll-like and NOD-like receptor activation. Notably, anergic platelet-depleted monocytes can be reactivated upon their replenishment with autologous platelets. Moreover, monocytes from patients with immune thrombocytopenia display naturally impaired cytokine responses, which were also reversed by platelet supplementation. Mechanistically, we show that the trans-cellular propagation of platelet p38 MAPK signaling through platelet vesicles licences the full cytokine responses of human monocytes. Our findings delineate platelets as paramount regulators of monocyte innate immune functions.

INTRODUCTION

Classical CD14⁺CD16⁻ monocytes make up ~85% of the circulating monocyte pool in humans. Compared to other subsets, classical monocytes are primed for programs involved in host defense, such as innate immune sensing of pathogens, phagocytosis, and display increased ability to secrete cytokines[1].

Monocyte-driven innate immune responses can reach different and extreme outcomes. While heightened monocyte activity triggers hyper-inflammation and cytokine storms[2-8], dysfunctional monocytes, on the other end of the spectrum, are involved in an equally life-threatening state of hypo-responsiveness, termed „immunoparalysis," which predisposes patients to opportunistic infections. Monocyte immunoparalysis is often observed after sepsis[9-11], major visceral surgery[9], and was recently associated with the severity of SARS-CoV-2 infections[12, 13]. Monocytes are also vital cells mediating "trained immunity", a series of long-lasting epigenetic and metabolic adaptations that enhance innate immune responsiveness upon subsequent encounters with pathogen molecules[14, 15]. Inappropriate monocyte activities may thus have life-long immunological consequences. The current SARS-CoV2 pandemic has evidenced how harmful aberrant[3-8] and dysfunctional[12, 13] monocyte activities can be and helped to raise the urgency to unravel the molecular mechanisms governing monocyte activity to new heights.

Here, we reveal a crucial role for platelets for the effector cytokine function of human monocytes. Blood monocytes continuously interact with platelets and form monocyte-platelet aggregates (MPAs) in a physiological state[16], which are increased in numerous inflammatory and thrombotic disorders[17-20].

Using different human monocyte isolation kits, we demonstrate that the amount of platelets in monocyte preparations directly impacts the cytokine output of freshly isolated CD14⁺ human monocytes. Removal of platelets from human monocytes caused a state of immunoparalysis marked by a transcriptional shutdown of pro-inflammatory genes, and an impaired capacity to secrete pro-inflammatory cytokines in response to Toll-like receptor (TLR) and Nod-like receptor (NLR) stimulation. Notably, both the transcription of pro-inflammatory genes and the release of the corresponding cytokines were reconstituted by the re-introduction of autologous platelets to platelet-depleted monocytes, demonstrating that platelet depletion causes a transient state of immunoparalysis in human monocytes. Furthermore, monocytes from patients with low blood platelet counts caused by immune thrombocytopenia (ITP), display a naturally impaired pro-inflammatory cytokine response. Remarkably, we demonstrate that the supplementation of ITP monocytes with healthy platelets "awakens" thrombocypenic monocytes from their anergic state, and restores their cytokine responses to levels equivalent to healthy competent monocytes.

While investigating the mechanisms by which platelets regulate cytokine production on monocytes, we discovered that platelets directly supply monocytes with functional p38 MAPK signaling through platelet-derived vesicles. Blocking p38 MAPK signaling on human platelets extinguished their ability to rescue the cytokine responses of platelet-depleted monocytes. Moreover, supplementation with fresh platelets can bypass p38-inhibition in human monocytes and restore their impaired cytokine secretion in a platelet:monocyte ratio dependent manner. Hence, our study reveals that the propagation of p38 MAPK signaling from platelets to monocytes regulates the pro-inflammatory activity of monocytes, and supports the clinical use of platelet supplementation to counteract monocyte immunoparalysis.

Our findings also challenge the idea that monocyte immune functions are autonomous, and uncover their dependency on platelets for their full pro-inflammatory cytokine capacity. These findings have important implications for our understanding of overactive monocyte-driven hyper-inflammation or dysfunctional monocyte cytokine responses.

RESULTS

Platelets are essential for the TLR- and NLR-induced secretion of pro-inflammatory cytokines by human monocytes.

Inflammasome activation and pyroptosis of human monocytes is associated with hyper-inflammation and overproduction of pro-inflammatory cytokines[8, 21]. We have recently shown that platelets boost the inflammasome activation of innate immune cells. We showed that monocyte-derived human macrophages display enhanced inflammasome activity and secrete higher levels of IL-1 cytokines when co-cultured with autologous and heterologous platelets[22]. To investigate the inflammasome-driven cytokine response of human monocytes we performed immune-magnetic isolation of classical (CD14⁺CD16⁻) monocytes from human blood. As previously demonstrated[22-24], isolated, untouched monocytes (referred hereafter as "standard monocytes", StdMo) contained a significant number of free (CD14⁻CD41⁺) and monocyte-platelet aggregates (CD14⁺CD41⁺) (**Figure S1A-D**). Removal of platelets from StdMo using a kit-provided platelet-depleting antibody enriched platelet-free monocytes (CD14⁺CD41⁻ cells) from

from 5.4% to 30.5% and decreased the percentages of free platelets from 94.6 to 69.5% (**Figure S1A-B**, n = 50), while monocyte counts remained constant (**Figure S1C**). Importantly, platelet-depleted monocytes (PdMo) remained viable in resting conditions and after stimulation with lipopolysaccharide (LPS) (**Figure 1A**). The LPS-triggered secretion of IL-6 and TNFα was virtually abolished in PdMo compared to StdMo, which contained platelets (**Figure 1B** and **S1D**). Removal of platelets also impaired the inflammasome-response of human monocytes, assessed by measuring the release of IL-1β in response to nigericin (Nig), a potent activator of the NLRP3 inflammasome (**Figure 1B**, and **S1E**). The impaired capacity of PdMo to secrete these cytokines was rescued by adding back autologous platelets (PdMo + Plts) at a ratio of 100 platelets per monocyte (**Figure 1B - 1C**, and **S1E**), which is close to physiological counts in healthy blood[25]. Importantly, none of the measured cytokines were secreted

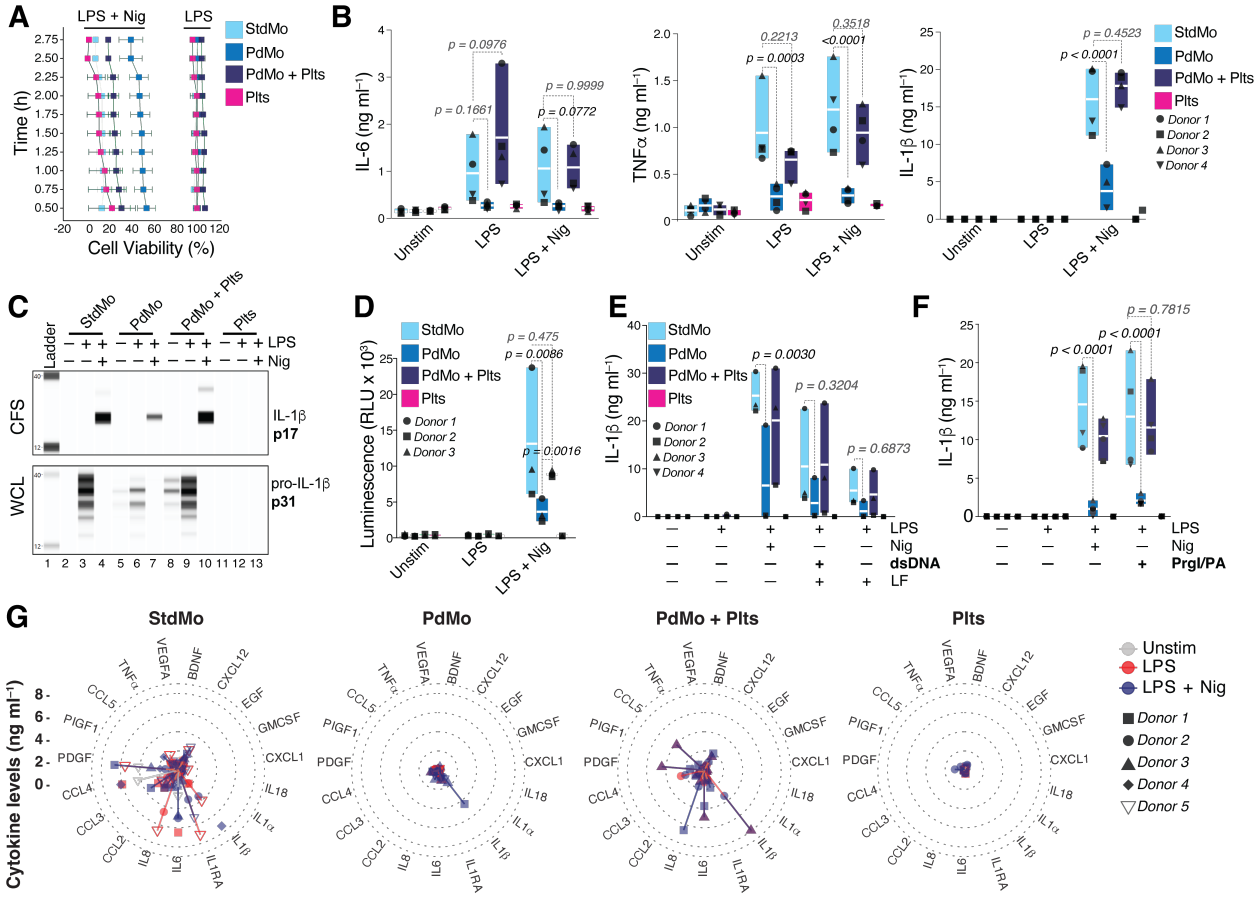

Figure 1. Platelets regulate the cytokine secretion of human monocytes.

(**A-B**) Cell viability assessed every 15 min and (**B**) concentrations of IL-6, TNFα, and IL-1β released into the cell-free supernatants (CFS) by untouched (StdMo, light blue), platelet-depleted (PdMo, blue), or PdMo that were supplemented with autologous platelets (PdMo + Plts, dark blue) at a 100:1 platelet:monocyte ratio. Cytokine levels secreted by platelets alone (Plts, purple) were measured as control. Cells were stimulated with LPS (2 ng ml^{-1} for 3h) followed by activation with nigericin (10 μM for 1.5 h).

(**C**) Intracellular maturation and secretion of IL-1β assessed by WES capillary electrophoresis coupled with Ab-based detection in whole cell lysates (WCL) or CFS of primary human monocytes stimulated as in **A**.

(**D**) Fluorometric assessment of caspase-1 activity in the CFS of primary human monocytes stimulated as in **A**.

(**E - F**) IL-1β concentrations in CFS of LPS-primed StdMo, PdMo, or PdMo + Plts that were transfected with Lipofectamin (LF) containing (**E**) double-strand DNA (dsDNA, 0.5 μg ml−1) for the activation of the AIM2 inflammasome. In (**F**), cells were treated with PrgI (100 ng ml^{-1}) and protective antigen (PA, 1 μg ml^{-1}) for 90 min, for the activation of the NLRC4 inflammasome. Floating bars display the max/min values with indication for the mean (white bands). Each symbol represents one independent experiment or blood donor.

(**G**) Radar plots displaying the top 19 highest cytokines detected by Cytokine Luminex in the CFS of human monocytes and platelets stimulated as in **A**. Protein concentrations are represented by the spread from inner (0 ng ml^{-1}) to outer circles (≥ 10 ng ml^{-1}). Colors represent stimuli (Grey: Unstim, Red: LPS, dark blue: LPS + Nig). Each symbol represents one independent experiment or blood donor (n = 5 for monocytes, and n = 2 for platelets alone). For better visualisation, cytokine concentrations (y axis) are displayed with a cut off at 8 ng ml^{-1}. Levels of IL-1RA and CCL4 reached 20 ng ml^{-1}. **See also Figure S1 and S2**.

by platelets alone (Plts), indicating monocytes as their primary source.

As expected[26], nigericin-induced activation of the NLRP3 inflammasome resulted in caspase-1 mediated pyroptosis, as demonstrated by a ~80% reduction in the viability of treated cells (**Figure 1A**), and the presence of active caspase-1 in the culture supernatants (**Figure 1D**). Consistent with a suboptimal inflammasome activation, platelet removal additionally reduced caspase-1 activity measured in the culture supernatants (**Figure 1D**), and the intracellular maturation of IL-1β (**Figure 1C** and **S1E**), while increasing the viability of nigericin-treated PdMo to ~60% (**Figure 1A**). Supporting the requirement of platelets for full inflammasome activation of human monocytes, platelet supplementation restored the activity of caspase-1 as well as the maturation and release of IL-1β (**Figure 1C** and **S1E**), and diminished the resistance of PdMo to nigericin-induced pyroptosis (**Figure 1A**).

In human monocyte-derived macrophages (hMDMs), platelets specifically license NLRP3 mRNA and protein expression, boosting the activation of the NLRP3 inflammasome[22]. To investigate if platelets regulate the activation of other inflammasomes in human monocytes, we assessed the impact of platelet depletion on the activation of AIM2 (**Figure 1E**) and NLRC4 (**Figure 1F**). Platelet depletion from monocytes directly influenced their ability to release IL-1β in response to AIM2 and NLRC4 activation (**Figure 1E-F**), indicating that, unlike hMDMs, the influence of platelets on monocytes is not restricted to the NLRP3 inflammasome. These findings suggest that platelets have a broader effect on the innate immune function of monocytes. Supporting this conclusion, platelet removal also impacted the monocyte production of IL-6 and TNFα in response to LPS (**Figure 1B** and **S1E**) and when other TLRs were used for stimulation (**Figure S1F**). We, therefore, investigated the impact of platelet depletion on the production of 45 human cytokines, chemokines, and growth factors in response to TLR4 and NLRP3 inflammasome activation (**Figure 1G**) or TLR1/2 and TLR7/8 activation (**Figure S1G**). While StdMo released copious amounts of pro-inflammatory cytokines including IL-1β, IL-6, CCL2, CCL4, IL-8, PDGF, and IL-1RA (> 10 ng ml^{-1}), the overall cytokine response of platelet-depleted monocytes (PdMo) was blunted. Yet, responses were mostly restored by replenishment with autologous platelets (50:1 platelet:monocytes) (**Figure 1G** and **S1G**). Hence, the disruption of cytokine responses of PdMo was not exclusive to TLR4 or the NLRP3 inflammasome or IL-1 cytokines, but revealed a similar state of immunoparalysis with broader impairment of monocyte cytokine responses to pattern recognition receptors (PRRs). Together, these findings demonstrate a paramount role of platelets for the TLR- and NLR-induced cytokine response of human monocytes.

The amount of platelets in preparations of human monocyte correlates with cytokine output.

Our results demonstrate a broad impairment of cytokine response of blood monocytes upon removal of platelets, which may be influenced by the chosen isolation method. Immunomagnetic separation of monocytes from human and mouse peripheral blood is a widely employed method to study primary immune cells in different experimental settings. Isolation can be achieved by positive selection, with anti-CD14 monoclonal antibodies (mAbs) coupled to magnetic beads, or negative selection with a cocktail of antibodies against unrelated blood cells, yielding “untouched" monocytes. To validate our findings using an additional isolation method, we compared the cytokine responses of monocytes isolated with the two most popular positive and negative isolation kits (**Figure S2**, and Methods). We found that positive selection (Miltenyi Biotech) of $CD14^+$ blood monocytes yielded cells of higher purity compared to the negative selection (STEMCELL™ Technologies) (**Figure S2B-C**). Positively-selected StdMo contained fewer platelets (**Figure S2B-C**), and responded poorly to TLR and inflammasome stimulation compared to negatively-isolated StdMo (**Figure S2C-D**). Cytokine levels secreted by positively-selected monocytes were comparable to negatively-selected monocytes after the platelet depletion step (i.e. PdMo) (**Figure S2C-D**). Importantly, despite the requirement of CD14 for LPS recognition, the impairment of CD14-positively-selected monocytes was not due to the engagement of CD14 by anti-CD14 magnetic beads[23], as these cells also displayed reduced cytokine response to Pam3CysSerLys4, a synthetic TLR1/2 ligand. Notably, the re-addition of autologous platelets to positive-selected monocytes boosted their cytokine responses (**Figure S2C-D**). These findings conclusively demonstrate that the presence of platelets in monocyte preparations directly impacts the cytokine output of human monocytes, and exclude that the effects we observed were due to a specific isolation method. Hence, the isolation method and the purity of cell preparations have broader effects on monocyte functions, and should be taken into account when interpreting results of *ex vivo* stimulation of human monocytes. To gain experimental flexibility in manipulating platelet and monocyte numbers, we employed negative selection

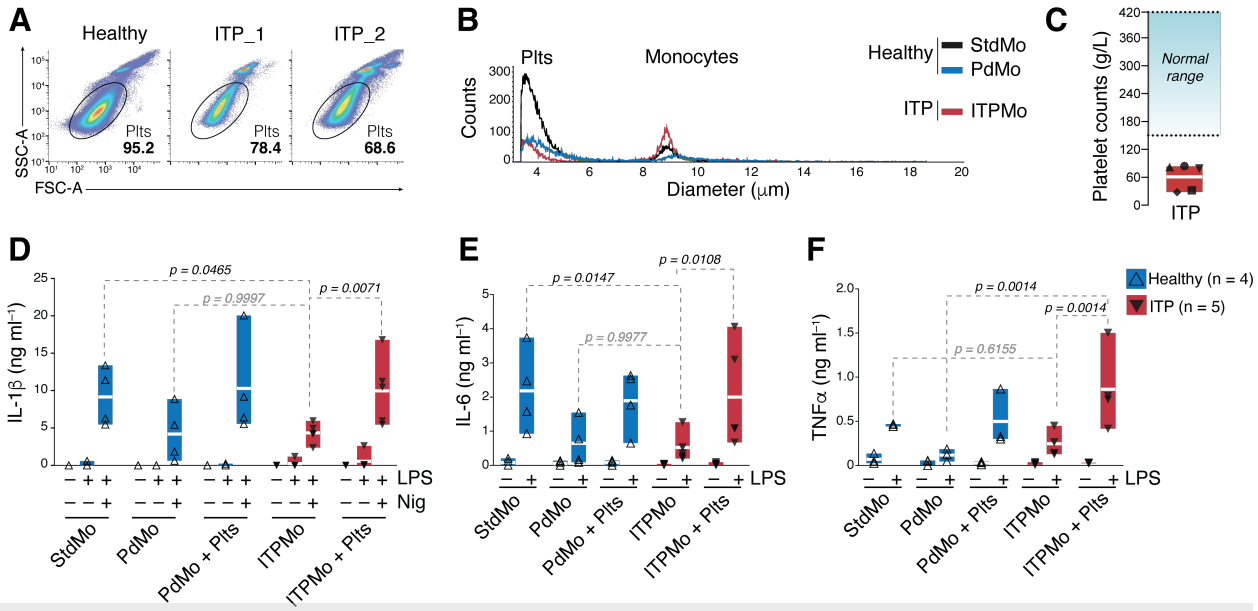

Figure 2. Platelet supplementation reverts immunoparalysis of ITP monocytes.

(**A**) Representative Flow Cytometry percentages and (**B**) CASY automated cell quantification of monocytes and platelets in preparations of untouched or platelet-depleted monocytes from healthy donors (± platelet-depletion) or untouched monocytes from ITP patients (ITPMo).

(**C**) Clinical laboratory quantification of platelets in the peripheral blood of ITP patients. Known healthy reference values are displayed for illustration purposes.

(**D-F**) Concentrations of IL-1β, IL-6 and TNFα released into the CFS by untouched (StdMo), and PdMo isolated from healthy volunteers (n = 4), or untouched monocytes from ITP patients (ITPMo, n = 5). Healthy platelet-depleted monocytes (PdMo + Plts), or ITPMo were supplemented with platelets (ITPMo + Plts). Cells were stimulated with LPS (2 ng ml^{-1}) for IL-6 and TNFα measurements, or LPS + Nig (10 μM) for IL-1β measurements. Data is displayed as floating bars with the max/min values and mean (white bands). P values were calculated with 2-Way Anova, Tukey's multiple comparison test, and are displayed in the figure. Each symbol represents one independent experiment or blood donor.

throughout our experimental settings and used the platelet removal step when indicated.

Platelet supplementation reverses inherent impaired cytokine responses of thrombocytopenic monocytes.

To assess the impact of platelets on the effector functions of monocytes in a real clinical setting − where blood platelet counts are inherently low − we isolated monocytes from patients with Immune Thrombocytopenia (ITP). ITP is an autoimmune disorder characterized by abnormally low blood platelet counts in the absence of other known causes of thrombocytopenia[27]. ITP patients recruited in this study were asymptomatic, but presented with low blood platelet counts (< $100x10^9$/L) (**Figure 2A-C**, and **Table 1**, Methods). Furthermore, blood leukocyte counts and plasma C-reactive protein concentrations were within normal ranges, and other co-infections were excluded (**Table 1**, Methods). Compared to monocytes isolated from healthy volunteers (StdMo), untouched ITP monocytes (ITPMo) were naturally impaired in their capacity to produce IL-1β in response to stimulation with LPS + Nig (**Figure 2D**), and IL-6 in response to LPS (**Figure 2E**). TNFα concentrations were also lower in LPS-stimulated, ITPMo. However, the differences did not reach statistical significance (p = 0.6155) (**Figure 2F**). Cytokine levels in ITPMo were comparable to the low amounts secreted by stimulated PdMo from healthy donors (**Figure 2D-F**). Strikingly, the re-addition of healthy platelets to ITPMo boosted all cytokine responses to levels comparable to healthy StdMo (**Figure 2D-F**), demonstrating that dysfunctional ITP monocytes can be reactivated by platelet supplementation. Together, these findings confirm that the observed effects of platelets on monocytes are not due to the manipulation of platelets during magnetic isolation, and demonstrate the clinical relevance of platelets in monocyte-driven immune responses in ITP. Furthermore, we show that platelet supplementation can overcome the impaired pro-inflammatory cytokine response of ITP monocytes.

Platelets are required for the LPS-induced pro-inflammatory transcriptional response of human monocytes.

The reversible nature of the cytokine impairment of PdMo in our experimental settings, and naturally occurring in ITP monocytes, suggests that the same signaling pathways that are shut down on PdMo are reactivated when platelets are reintroduced. To gain insights into the transcriptional landscape of human monocytes subjected to

platelet depletion/supplementation, we assessed the expression of 770 genes encompassing the myeloid innate immune response in untouched (StdMo), platelet-depleted (PdMo), or PdMo that were replenished with 50:1 autologous platelets (PdMo + Plts). Monocytes were assessed in resting conditions (Unstim), or after *ex vivo* stimulation with LPS or LPS followed by nigericin stimulation (**Figure 3**).

We first compared the transcriptional effects of stimulation with LPS or LPS + nigericin in StdMo, PdMo, PdMo + Plts, and Plts. A principal component analysis (PCA) revealed that the transcription profile of platelets vs. monocytes accounted for 43% of the variation among the samples (PC1, **Figure 3A**). Indeed, platelet transcripts formed separate clusters distant from monocytes, and did not show a distinguishable transcriptional response to stimulation (**Figure 3A**, Plts, pink symbols), in line with a negligible contribution of platelet transcripts to the overall mRNA pool. The second source of variation (PC2) was related to the stimulation of human monocytes. Unstimulated StdMo (green circles) were distantly scattered from stimulated conditions (LPS: green squares; and LPS + Nig: green triangles) (**Figure 3A**). Notably, stimulated PdMo displayed a less distinguishable transcriptional profile (compare red circles to red squares or triangles). Furthermore, all PdMo samples clustered in proximity to unstimulated StdMo (Green circles, **Figure 3A**), indicating a loss of transcriptional response to stimulation. Importantly, the re-addition of autologous platelets to PdMo (50:1 ratio) partially restored the

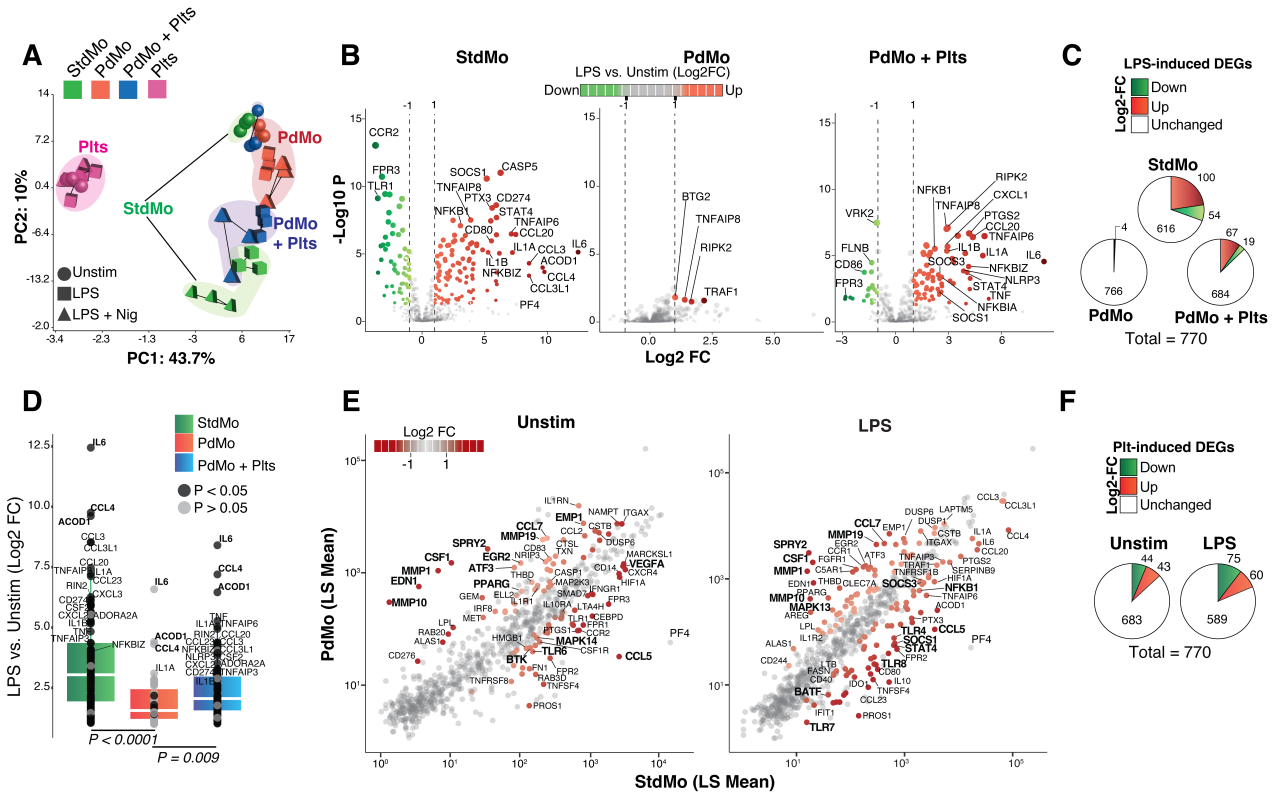

Figure 3. Platelet depletion/supplementation dynamically governs gene expression of human monocytes.

(**A**) Principal Component Analyses (PCA) of gene expression in StdMo (green), platelet-depleted monocytes (PdMo, red), platelet-depleted monocytes reconstituted with platelets (PdMo + Plts, blue), and platelets alone (Plts, pink). Each symbol represents one donor. Stimulations are represented with shapes (elypse = unstimulated, square = LPS, triangle = LPS + Nig).

(**B**) Volcano plots showing log2 fold change (x-axis) and significance (−log10 *p-value; y-axis) of genes differentially expressed comparing LPS-stimulated vs. unstimulated (Unstim) StdMo, PdMo, or PdMo + Plts.

(**C**) Pie charts indicate the number of up- and downregulated DEGs in each group upon LPS stimulation.

(**D**) Quantitative expression (Log2 Fold Change) of the LPS-induced (>= 2 Fold Change) genes in StdMo (green), PdMo (red) or PdMo + Plts (blue).

(**E**) Scatter plots displaying the log2 fold change (x-axis) of StdMo vs PdMo (y-axis) from DEGs comparing the effects of platelet removal in Unstim and LPS-stimulated conditions. DEGs with 2-Fold change are highlighted in red.

(**F**) Pie charts representing the DEGs of the comparisons in **D**, representing DEGs induced by platelet depletion in unstimulated or LPS-stimulated monocytes.

transcriptional response to stimulation as indicated by the separation of the unstimulated PdMo + Plts samples from the stimulated areas, and approximating them to the transcriptional profile of stimulated StdMo (**Figure 3A**, blue symbols).

Platelet depletion also markedly impacted the LPS-induced transcriptional landscape of monocytes. LPS stimulation in StdMo changed the expression of 154 genes (100 up-regulated and 54 down-regulated), when compared to the unstimulated conditions (**Figure 3B-C**). In sharp contrast, only four genes were significantly induced by LPS (FoldChange ≥ 2, p< 0.05) in PdMo (**Figure 3B-C**), indicating a general "shut-down" of inflammatory gene expression. Notably, the re-addition of autologous platelets to PdMo restored the expression of 86 genes (67 up and 19 down) (**Figure 3B-D**), quantitatively resembling the profile of StdMo (**Figure 3D**). These results are in agreement with the multiplex cytokine analysis (**Figure 1G** and **S1F**).

Next, to specifically address the effects of platelet depletion/replenishment on monocytes, we separately compared StdMo vs. PdMo in unstimulated and stimulated conditions (**Figure 3E-F**). Irrespective of LPS stimulation, platelet depletion *per se* altered the expression of 87 genes in steady-state (unstimulated) monocytes (**Figure 3E-F**). In the absence of platelets, genes involved in pro-inflammatory signaling such as mitogen-activated protein kinase 14 (*MAPK14*, or p38α), and Bruton's tyrosine kinase (*BTK*) were down-regulated. In contrast, numerous transcription factors (TFs) involved in monocyte-differentiation processes, DNA methylation, or repressors of NFκB signaling were induced. Interestingly, detailedinspection of the most highly differentially expressed genes (DEGs) identified several regulators of monocyte cytokine function. For example, genes involved in the sensing of chemokines or external stimuli (e.g., *CCR2*, *FCGR3A*, and *CD14*) were down-regulated in PdMo. In contrast, several TFs (e.g., *EGR2*, *PPARG*) and nuclear factor κB (*NFκB*) and ERK-MAPK repressor genes (e.g., *ATF3* and *SPRY2*) were up-regulated (**Figure 3E-F**). These findings demonstrate that transcriptional reprogramming underlies the functional effects of platelet depletion in primary human monocytes. Furthermore, in line with the cytokine secretion, the transcriptional shut-down of pro-

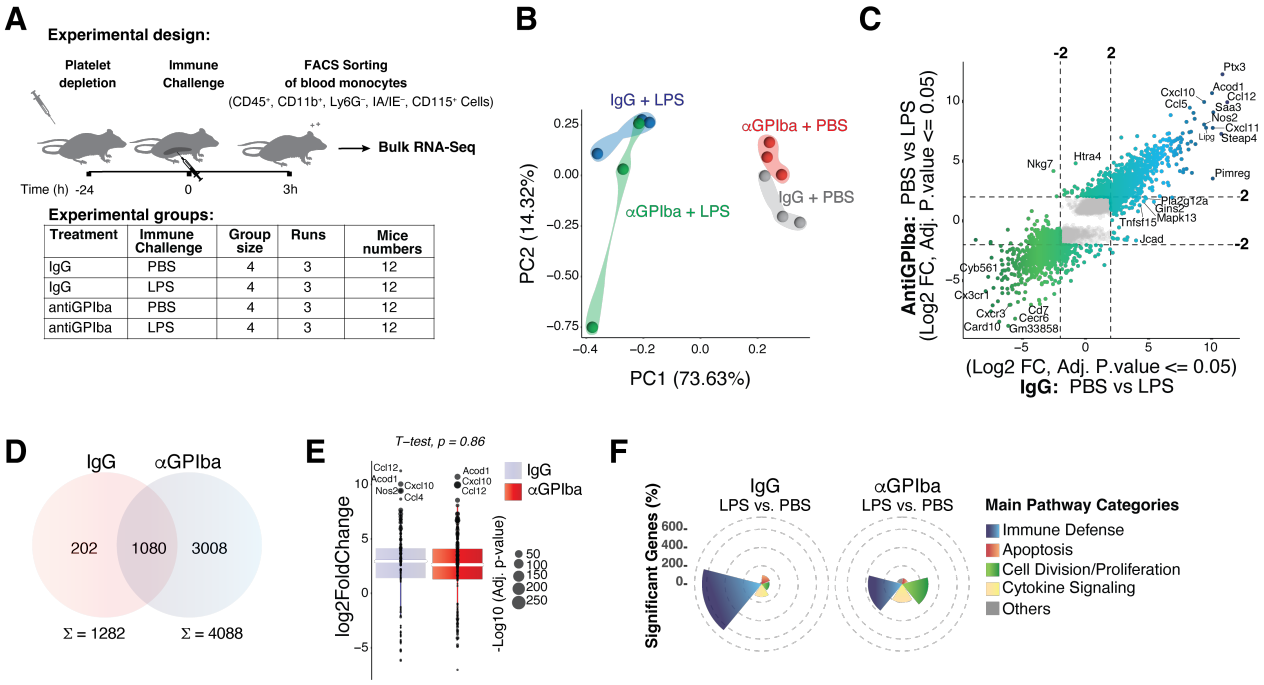

Figure 4. Platelet depletion in vivo does not affect mouse monocyte functions.

(**A**) Schematic representation of the experimental setting for platelet depletion *in vivo* depletion followed by intravenous challenge with LPS, FACS-sorting and bulk-RNASeq of blood monocytes. Monocytes were isolated from PBMCs from pooled blood of 4 mice per group (IgG- or anti-GPIbα-treated) each challenged either with LPS or PBS in 3 different experiments.

(**B**) PCA analysis showing the variation of transcripts in isolated monocytes from IgG or antiGPIbα-treated mice challenged with LPS, or vehicle (PBS).

(**C**) Scatter plot comparing the DEGs (-2 <= Fold Change >= 2, FDR corrected P.value < 0.05) of LPS-induced gene expression in monocytes isolated from IgG-treated (x.axis) vs. anti-GPIbα-treated mice (y.axis).

(**D**) Fold change of the 190 DEGs characterized as related to immune defense that were induced by LPS in monocytes from IgG vs. antiGPIbα-treated mice.

(**E**) Main represented categories of pathways (GO analysis) from the DEGs induced by LPS on monocytes from IgG-treated vs. platelet-depleted mice. See also **Figure S3**.

inflammatory gene expression in PdMos can be reversed by their replenishment with fresh platelets.

The requirement of platelets for the pro-inflammatory transcriptional response to LPS is not recapitulated in mice.

Our results in ITP patients demonstrate that monocytes from thrombocytopenic individuals display naturally impaired cytokine responses to TLR and NLR activation. To recapitulate these findings *in vivo* and investigate the underlying mechanisms, we induced thrombocytopenia in mice by i.v. injection of 2 mg/kg of body weight of a rat anti-glycoprotein Ibα (GPIbα) mAb or, as control, with equal amounts of a rat IgG isotype[28, 29]. We then challenged platelet-depleted mice with i.v. injection of LPS (2 mg/kg). Antibody-dependent platelet clearance was efficient to lower blood platelet counts in treated mice (**Figure S3A**). However, differently to human monocytes and confirming previous observations of LPS injections in platelet-depleted mice[28, 30], platelet depletion did not singficantly influence the plasma levels of IL-1β, TNFα and IL-6 in challenged mice (**Figure S3B**).

To investigate the effects of platelet depletion specifically on blood monocytes, we performed RNASeq analysis on FACS-sorted (Ly6G$^-$ IA/IE$^-$ CD45$^+$ CD11b$^+$ CD115$^+$) murine PBMCs (**Methods**, and **Figure 4A**). Contrasting the results of PCA in human monocytes (**Figure 3A**), PCA-based clustering demonstrated that more than 70% of the transcriptional variance in murine monocytes was related to their stimulation with LPS, rather than the effects of platelet depletion, which accounted for 14% of the variance (**Figure 4B**). Consistent with the removal of platelets by anti-GPIbα mAbs, the expression of several platelet transcripts (e.g., *Pf4*; *Gp9*; *Itga2b*, *Ppbp*, *Tubb1*, *Treml1,* and *Clu*) was down-regulated in monocytes from platelet-depleted compared to IgG-treated mice in the absence of immune stimulation (PBS group) (**Figure S3C**). Nevertheless, platelet depletion increased the expression of genes involved in the complement cascade (e.g. *C1qa*, *C1qb,* and C1qc), and in cell activation processes (e.g. *Htra3* and *Mertk*) (**Figure S3C**), correlating with enrichment in pathways involved in blood coagulation, hemostasis, platelet activation, complement and wound healing processes (**Figure S3D**).

Having demonstrated a signature for the platelet depletion on the transcriptional landscape of FACS-sorted mouse monocytes, we next compared the effects of platelets on the monocyte transcriptional response to LPS challenge *in vivo*. Expression profiling analysis (**Figure S3E**) and gene ontology (GO) (**Figure S3F**) confirmed that monocytes isolated from IgG-treated mice displayed a typical LPS-induced transcription profile[31] with the enrichment of genes involved in immune defense among the highest DEGs (e.g. *Cxcl10*, *Ccl12, Il1a, Ly6c,* interferon-stimulated genes (ISGs), and *Il12a*) and the concomitant and expected dow-regulation of *Card10 and Cx3cr1*[32] (**Figure 4C**). Overall, LPS stimulation altered the expression of more transcripts in monocyte from platelet-depleted (anti-GPIbα-treated) compared to IgG-treated mice (4088 vs. 1282 transcripts, **Figure 4D**). However, the expression of the 1080 LPS-induced genes was comparable between anti-GPIbα and IgG-treated mice (**Figure S3E**). More than 80% of the LPS-induced gene signature was shared between monocytes from IgG-treated and platelet depleted mice, while 3008 DEGs exclusively expressed in monocytes from platelet-depleted mice, and 202 DEGs being exclusively regulated in monocytes from IgG-treated mice (**Figure 4D**). Furthermore, a direct comparison of the expression levels (log2FoldChange) of 190 genes involved in immune defense programs that were regulated by LPS confirmed no significant differences in their expression between IgG and anti-GPIbα-treated mice (**Figure 4E**), contrasting the transcriptional changes observed in human PdMo (**Figure 3B-D**). Nevertheless, the LPS-induced expression profiles identified a higher enrichment scores for pathways involved in host immune defense programs in IgG-treated mice (e.g. immune response to virus, immune system processes, cellular responses to IFNβ, and inflammation, **Figure 4F** and **S3F**). These pathways were also represented, but with lower enrichment scores in the gene profile of platelet-depleted mice, which was skewed towards apoptosis and cell cycle regulation (**Figure 4F** and **S3F**). These differences may be related to the higher number of LPS-induced transcripts detected in platelet-depleted vs. IgG-treated monocytes (**Figure 4D**). From these results, we conclude that, althouth platelets alter the LPS-induced transcriptional landscape of murine monocytes, highlighinh pathways involved in cell cycle and division, the pro-inflammatory profile was comparable between platelet-depleted and IgG-treated mice.

Platelets are cellular sources of active kinases

Overall, our transcriptomic approach indicated that platelets influence the expression of several genes involved in key signaling pathways that orchestrate pro-inflammatory cytokine production in monocytes, such as NFκB, BTK, and MAPK. We therefore used a bait peptide chip array to dynamically monitor the activity of signaling pathways triggered by the interaction of platelets with human

monocytes from five different donors. We profiled the activation of serine/threonine (STK) and protein tyrosine (PTK) kinase networks on primary human untouched monocytes (StdMo), PdMo, or PdMo replenished with platelets (PdMo + Plts) as well as on platelets alone (Plts). We observed that the removal of platelets markedly impacted the kinome network of monocytes (**Figure 5A-D** and **S4A**). PdMo showed a very distinct profile of activated PTKs and STKs compared to StdMo (**Figure 5B** and **5C**). With few exceptions, the phosphorylation status of all PTK substracts, and numerous STK substracts, were significantly lower in PdMos compared to StdMo (**Figure 5C-D**). Supporting the results of mRNA expression (**Figure 3**), platelet depletion decreased the activity of BTK, p38 MAPK, and of additional kinases, such as MAPK-activated protein kinases (MAPKAPK), IKK kinases, erythropoietin-producing human hepatocellular receptors (Eph), Cyclin-depended kinases (CDK), protein kinase A, (PKA) and protein kinase C (PKC). In contrast, platelet depleted monocytes displayed increased activation of Janus kinases (JAKs) and IKKs, which are known regulators of NFκB signaling [33](**Figure 5A**). In line with the altered function of these groups of kinases, pathway analysis revealed that platelet depletion predominantly altered the activity of kinases involved in signal transduction associated with NFκB activation, immune responses via CD40 signaling, MAPK, and JAK/STAT signaling pathways (**Figure 5E**). The tyrosine kinases of the CMGC family, which includes CDKs,

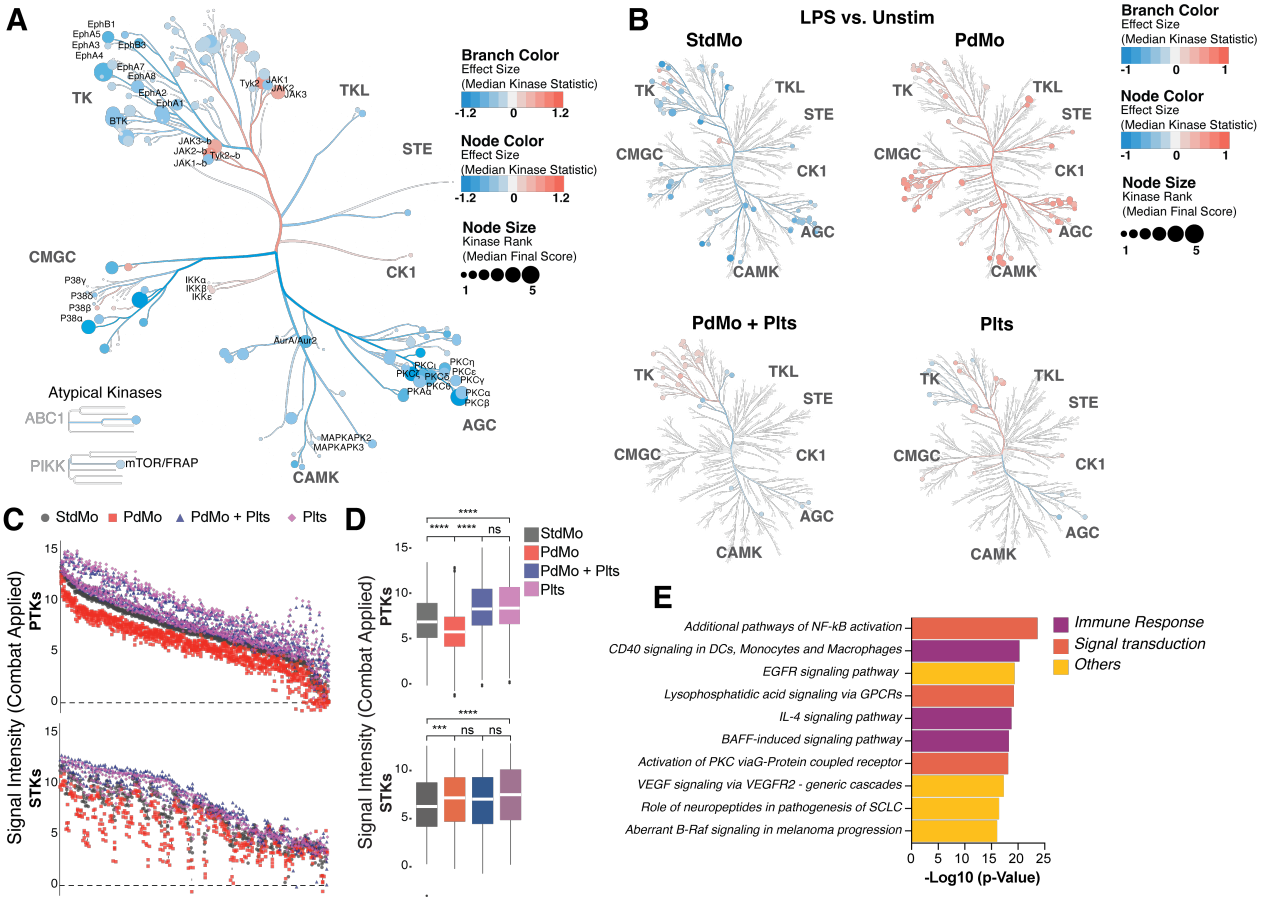

Figure 5. Platelets are cellular sources of MAPKs and transcription factors.

(**A-B**) Coral trees display the activity of Protein Tyrosine (upper branches) and Serine/Threonine kinases (lower branches) in StdMo, PdMo, PdMo + Plts and platelets upon LPS stimulation for 15 min measured with a PamStation12 (PamGene). (**A**) Impact of platelet depletion on the activity of PTK and STK in unstimulated monocytes. (**B**) Effects of LPS stimulation on the activation of PTKs and STKs in StdMo, PdMo, PdMo + Plts and platelets. Red: increased kinase activity, Blue: reduced kinase activity.

(**C-D**) Scatter plots and **D** box plot showing the signal intensity for the phosphorylation status of phosphosites (x.axis) that are substracts of PTK (top) and STK (bottom) comparing StdMo, PdMo, PdMo + Plts, and platelets alone (Plts). Each symbol shows one donor (n = 5) and only include peptides which passed the QC. batch correction with a 2-step Combat correction. P values in D were calculated by Anova multiple comparison.

(**E**) Pathway analysis of the most represented signaling pathways dinamically changed upon platelet depletion/re-addition to primary human monocytes. See also **Figure S4**.

MAPKs, glycogen synthase kinases (GSKs) and CDC-like kinases (CLKs) figured among the kinases most dynamically changed by platelet depletion and re-addition. Within the STK group of kinases, the 5 top phosphosites that showed a 2-fold change between StdMo and PdMo, irrespective of LPS stimulation, were the ETS transcription factor ERF (P50548), which is a substrate of CKDs and MAPK[34]; the Potassium voltage-gated channel subfamily A member 1 (KCNA1, Q09470); and Annexin A1 (P04083), which is phosphorylated by CKD, MAPKs, and PKC and promote the expression of pro-inflammatory cytokines[35]. Combined, the transcriptome (**Figure 3**) and kinome (**Figure 5**) of human monocytes subjected to platelet depletion/re-addition revealed dysregulation of key cytokine-regulatory pathways in PdMo.

Supporting that platelets regulate the NFκB activity on monocytes, addition of increasing concentrations of platelets increased TLR2-triggered NFκB activity in THP-1 monocytes encoding a NF-kB promoter reporter gene (**Figure S4B**). Interestingly, the kinase activity assay demonstrated a high basal kinase activity on platelets (**Figure 5C-D**). To confirm these results, we assessed the protein levels and phosphorylation status of two major cytokine-regulating pathways, NFκB and MAPK p38, on platelets and monocytes that were depleted/reconstituted with platelets. Confirming the dynamic changes in NFκB activation caused by platelet depletion/reconstitution in human monocytes, the LPS-induced phosphorylation of the NFκB subunit p65 (RelA) was impaired in PdMo, as measured by HTRF (**Figure S4C**) and immunoblotting (**Figure S4D**), and was restored by the re-addition of platelets (**Figure S4C-D**). Indeed, we observed pronounced phosphorylation of p65 (**Figure S4D**), and p38 MAPK on platelets (**Figure S4F**) in steady state. This was confirmed by assessing native and phosphorylated (P-)p65 and p38 in the lysates or supernatants of human platelets (**Figure S4E**

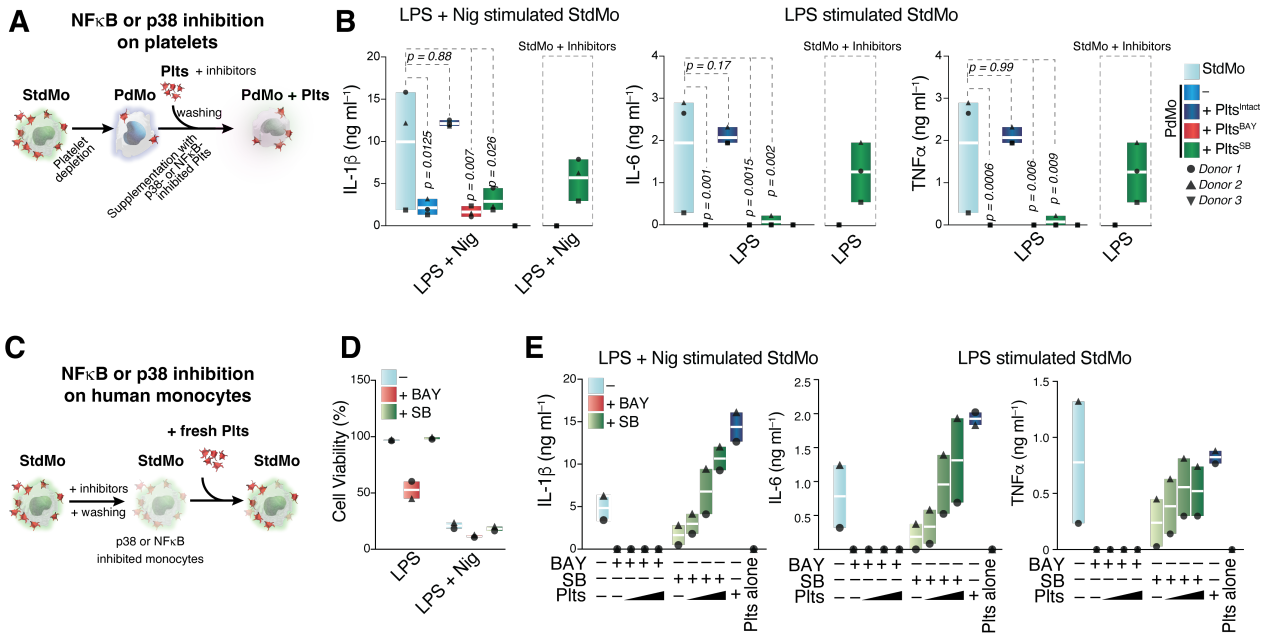

Figure 6: Platelets supply functional MAPK p38 signaling and reverse p38-inhibition on primary human monocytes.

(**A**) Schematic representation of the supplementation of platelet-depleted (PdMo) primary human monocytes with autologous platelets that were left untreated (+ Plts^{Intact}), or pre-incubated for 20 min with 50 µM of BAY 11-7082 to inhibit NFkB (+ Plts^{BAY}) or 20 µM of SB203580 to inhibit p38 MAPKs (+ Plts^{SB}) and washed before being added to PdMo.

(**B**) IL-1β, TNFα, and IL-6 concentrations in CFS of StdMo, PdMo, or PdMo that were supplemented with platelets pretreated with BAY11-7082 (+ Plts^{BAY}), SB203580 (+ Plts^{SB}), or left untreated (+ Plts^{Intact}). Co-cultures were stimulated with LPS (2 ng/ml) followed by nigericin stimulation (10 µM). Side graphs displays StdMo that were continuously treated with the inhibitors displaying the expected inhibitory capacity of the inhibitors to account for carry over throughout the assay.

(**C**) Schematic representation of the inhibition of NFkB or MAPK p38 on primary human monocytes (StdMo) followed by their replenishment with fresh autologous platelets.

(**D**) Cell viability assay in human monocytes treated with BAY 11-7082 (50 µM) or SB203580 (20 µM) followed by stimulation with LPS or LPS + Nig.

(**E**) IL-1β, TNFα, and IL-6 concentrations in the CFS of StdMo that were treated with BAY 11-7082 or SB203580 before been added with increasing ratios of freshly isolated platelets (1:5, 1:50, and 1:100). Cells were stimulated with LPS or LPS and nigericin (LPS + Nig) as in **A**. Floating bars display max/min values with indication to the mean (white bands). Each symbol represents one donor. **See also Figure S5.**

and **7A**). Although P-p65 was mostly enriched in platelets, P-p38 was additionally detected in platelet supernatants, indicating that platelets release this molecules. These results indicate that platelets have an additive effect on the induction of these signaling pathways in human monocytes. Together, these findings highlight the involvement of the NFκB and MAPK p38 signaling pathways as candidate mechanism by which platelets regulate the cytokine production of human monocytes.

Platelets supply p38 MAPK signaling that boosts the cytokine response of human monocytes.

Despite being anucleated, our results support independent observation that platelets contain cytoplasmic transcription factors[36-39], and signaling molecules such as p38 MAPK[40]. Given the abundance of these key cytokine regulating molecules in platelets and the corresponding dynamic activation of these pathways on platelet-depleted/ replenished monocytes (**Figures 3** and **5**), we speculated that platelets could be cellular sources that supply monocytes with these molecules.

Cell-to-cell propagation of transcription factors, MAP kinase, and other signaling molecules have been reported to occur through gap junctions between connecting cells, with biological functions demonstrated in recipient cells[41, 42]. However, little is know about trans-cellular propagation of signalling molecules when circulating cells adhere to one another. To address the requirement of platelet-derived NFκB and p38 for monocyte function, we specifically inhibited these molecules in platelets and used them to supplement platelet-depleted monocytes. For this, we pre-incubated platelets with an irreversible inhibitor of IKKβ phosphorylation BAY 11-7082 (BAY) or SB203580, an inhibitor of p38 MAPKs[43]. After washing away the inhibitors, we supplied PdMo with intact or inhibitor-treated platelets (**Figure 6A**). BAY blocked the thrombin-induced P-selectin expression on treated platelets (**Figure S5A-B**). Importantly, addition of intact platelets, but not NFκB- or p38-inhibited platelets, restored IL-6 and TNFα secretion of LPS-stimulated PdMo as well as LPS + nigericin-induced IL-1β production (**Figure 6B**). To account for inhibitor carry over, we separately treated monocytes with BAY or SB203580 (**Figure 6B**, last two bars showing 100% inhibition). While BAY completely abrogated monocyte cytokine responses to TLR and NLRP3 activation, direct incubation of monocytes with SB203580 partially inhibited their response. These findings support that p38 and NFκB or their downstream signaling in platelets is essential for the platelet-regulation of cytokine responses of human monocytes.

Next, we sought out to specifically address whether platelets supply NFκB or p38 to monocytes. To simulate a scenario, in which platelets would be the only cellular source of functional NFκB or p38, we examined whether supplementation with fresh platelets could bypass NFκB or p38 inhibition in primary human monocytes. To demonstrate this, we pre-incubated monocytes with BAY and SB203580. After washing the inhibitors away, we supplemented BAY- or SB203580-treated monocytes with growing concentrations of intact platelets freshly isolated from the same donors (**Figure 6C**). Consistent with dysfunctional NFκB and p38 signaling[44], BAY- and SB203580-treated monocytes were incapable of secreting cytokines in response to LPS, or LPS + Nig (**Figure 6E**). Strikingly, the addition of intact platelets dose-dependently bypassed p38-inhibition and restored cytokine secretion in SB203580-treated monocytes (**Figure 6E**). In line with previous observations of toxicity associated with BAY-11-7082 in human cells[45, 46], BAY-treated monocytes displayed decreased viability (**Figure 6D**) precluding us from further addressing the importance of platelet-derived NFκB. Hence, these findings support that platelet-supplementation restores dysfunctional p38 activity in p38-inhibited monocytes in a dose-dependent manner. Indeed, in contrast to intact platelets, SB203580-treated platelets failed to restore cytokine responses in SB203580-treated monocytes (**Figure S5C**). Altogether, these findings demonstrate that platelets supply functional p38 signalling required for the optimal cytokine responses of human monocytes, and reveal a novel layer of cell-to-cell communication in innate immunity.

Platelet-derived vesicles regulate cytokine secretion in human monocytes.

Next, we addressed the mechanisms by which platelets could supply signaling molecules to human monocytes. We have previously demonstrated that, in human macrophages, platelets regulate inflammasome activation in a contact-independent manner through the release of soluble mediators[22]. Furthermore, we detected P-p38 in supernatants of platelets, even after pelleting cells at 20.000 x g and assessing proteins in cell-free sups (**Figure 7A**). We therefore assessed whether the transfer of platelet-supernatants (Plts Sups) could reconstitute faulty cytokine production in stimulated platelet-depleted monocytes (PdMo). For this, we reconstituted PdMos with platelets or with supernatants of platelets submitted to different centrifugation forces (500 to 20,000 x g). Notably, platelet supernatants efficiently restored the cytokine secretion in LPS-stimulated PdMos (**Figure 7B**), indicating

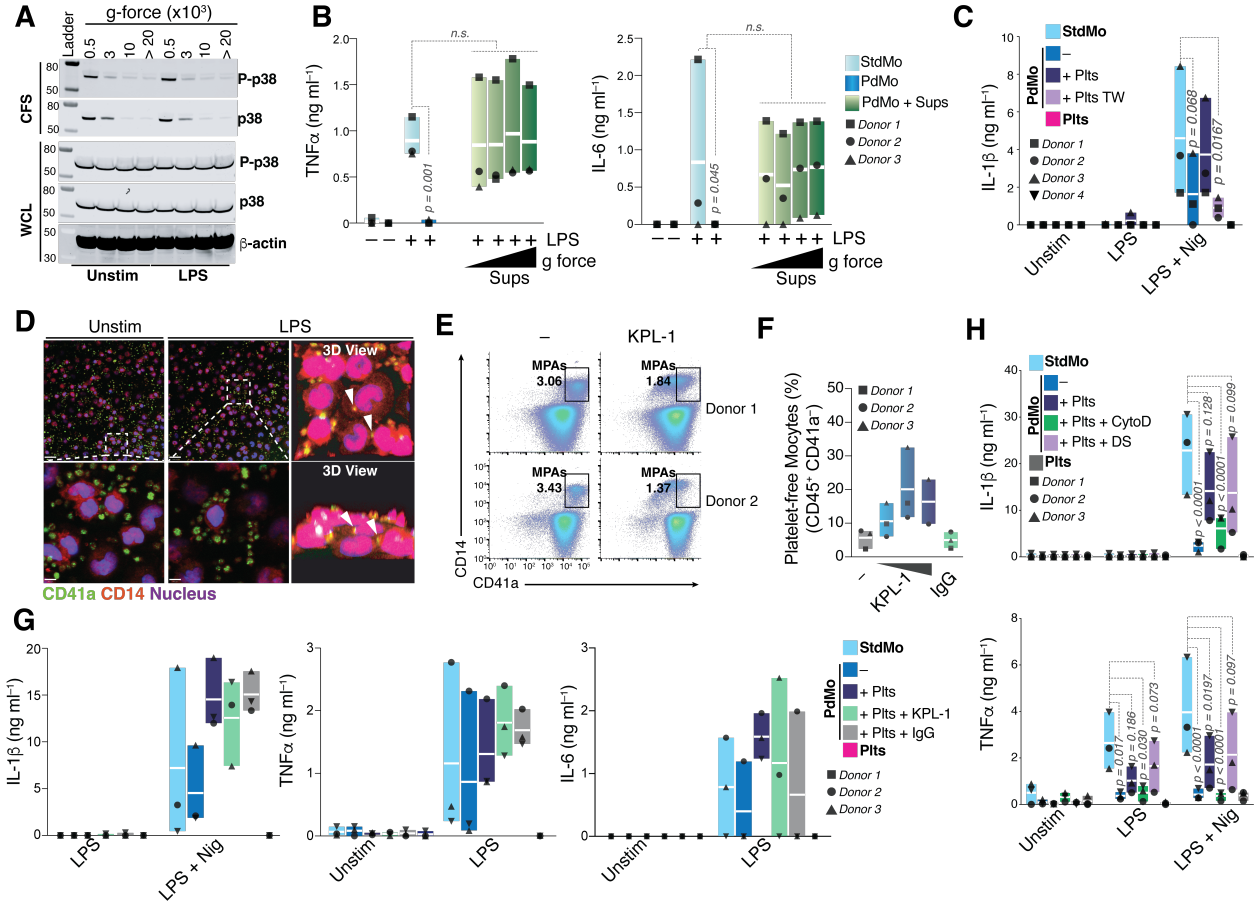

Figure 7. The platelet-monocyte crosstalk is contact dependent.

(**A**) Immunoblot of MAPK14 (p38) or phosphorylated MAPK14 (P-p38) in resting (Unstim) or LPS-activated (LPS) human platelets. Platelets were submitted to centrifugation at 500 x g, 3000 x g or 10,000 x g and the levels of MAPK14 were assessed in the pellets (WCL) or supernatants (CSF) after centrifugation. Results are representative of two independent experiments.

(**B**) Cytokine levels in CFS of StdMo, PdMo, and PdMo that were supplemented with CSF of platelets generated as in **A**.

(**C**) IL-1β levels in CFS of StdMo, PdMo, and PdMo that were supplemented with autologous platelets (PdMo + Plts) directly, or in trans-well separated by a 0.4 µm membrane. IL-1β were measured by HTRF and are represented as floating bar graphs. Additional cytokines are displayed in **Figure S6**.

(**D**) Confocal imaging of StdMo and platelets. Cells were stained with CD41a AF488 (platelets: green) and CD14 AF647 (monocytes: red). Nuclei were stained with Hoechst 34580 (blue). Scale: 24 µm (top panel); 4.8 µm (bottom panel). White arrows indicate points of contacts between platelets and monocytes. Images are from one representative of four independent experiments.

(**E**) Representative flow cytometry assessment and gating strategy of StdMo that were incubated with growing concentrations of KPL-1 (5, 10 or 25 µg ml^{-1}), or IgG (25 µg ml^{-1}). Gates indicate the frequencies of free platelets ($CD45^-$ $CD41a^+$), MPAs ($CD45^+$ $CD41a^+$) and platelet-free monocytes ($CD45^+$ $CD41a^-$). Data is representative of two independent experiments with several donors.

(**F**) Cumulative flow cytometry frequency of free monocytes ($CD45^+$ $CD41a^-$) in StdMo treated with growing concentrations of KPL-1 (5, 10 or 25 µg ml^{-1}), a specific mAb against P-selectin, or an unrelated isotype IgG control (25 µg ml^{-1}). See **Figure S4E** for gating strategy.

(**G**) IL-1β, TNFα and IL-6 levels released by stimulated StdMo that were treated with increasing concentrations of KPL-1 (5, 10 or 25 µg ml^{-1}), or IgG (25 µg ml^{-1}). Data is displayed as floating bars with the max/min values and mean (white bands). P values were calculated with 2-Way Anova, Tukey's multiple comparison test, and are displayed in the figure. Each symbol represents one independent experiment or blood donor.

(**H**) IL-1β and TNFα levels in CFS of StdMo, PdMo, and PdMo that were supplemented with autologous platelets (PdMo + Plts, 100:1 platelets/monocytes). Monocytes were pre-treated with Cytochalasin D (CytoD, 50 µM) or Dynasore (DS, 30 µM) before being supplied with Plts. Cells were stimulated with LPS (2 ng·ml^{-1}), followed by activation with nigericin (10 µM).

that platelets release molecules that mediate the platelet-effect on monocytes.

To address whether the molecules released by platelets were contained within vesicles, we employed trans-well assays. For this, PdMos were reconstituted with autologous platelets (PdMo + Plts) directly, or in trans-wells separated by a membrane with 0.4 µm pores. These experiments demonstrated that the re-addition of platelets directly to PdMo monocytes, but not in trans-wells, rescued most of the measured cytokines (**Figure 7C** and **S6A**). Taken

together, these findings rule out the involvement of soluble factors, and support that the platelet-monocyte crosstalk is mediated through vesicles larger than 0.4 µm. Supporting these conclusions, confocal imaging of the interaction of platelets with PdMos revealed numerous points of contacts between these cells (**Figure 7D**), however, no internalization of platelets was visualised.

Next, we sought to assess the dependency of ligand-receptor interaction between platelets and monocytes for the cytokine regulation in the latter. Monocyte-platelet binding is predominantly mediated by interactions between platelet P-selectin (P-sel, or CD62P), and P-selectin glycoprotein ligand-1 (PSGL-1, or CD162) on monocytes[24, 47]. We therefore tested whether blocking the P-sel-PSGL-1 interactions with KPL-1, a specific mAb against P-sel, prevents the ability of platelets to reconstitute the cytokine dysfunction of PdMos. Notably, KPL-1 but not an IgG control mAb dose-dependently dissociated monocyte-platelet aggregates (MPAs) in StdMo, generating platelet-free monocytes ($CD14^{+}CD41a^{-}$ cells) (**Figure 7E-F** and **S6D**). However, KPL-1 did not affected the production of pro-inflammatory cytokines on stimulated StdMos (**Figure 7G**). Furthermore, KPL-1 also did not prevent the ability of platelets to reconstitute cytokine dysfunction of PdMos (**Figure 7G**). These results indicate that the P-sel-PSGL-1 pairing is not involved in the induction of pro-inflammatory cytokines on monocytes. Nevertheless, the findings that KPL-1 prevented physical interactions between platelets and monocytes supports that other signaling mechanisms may be involved. Of note, both soluble and immobilized P-sel can regulate innate immune functions of stimulated monocytes[48], and platelets are known to shed P-sel vesicles[49]. However, the simulation of platelet-binding using soluble recombinant human P-sel (rhCD62P, P-sel) did not rescue the impaired secretion of cytokines by PdMo, compared to the re-addition of autologous platelets (**Figure S6E**). Together these findings indicate that platelets regulate cytokine production on human monocytes independently of the classical P-sel-PSGL-1 axis. Moreover, despite causing a physical separation of platelets and StdMo, KPL-1 can did not prevent the cytokine secretion, indicating the participation of vesicles, still be present in the well.

Finally, we investigated the mechanisms by which platelets or platelet-derived vesicles mediate the platelet-monocyte cross-talk. It is well-documented that macrophages, neutrophils, and monocytes phagocytose platelets[22, 50-52]. Although we were unable to visualize internalization of platelets by monocytes (**Figure 7D**), inhibition of actin polymerization in platelet-depleted monocytes (PdMo) using Cytochalasin D (CytoD) (**Figure 7H**) or Latrunculin B (Lat-B) (**Figure S6B**) disrupted the effects of platelet re-addition to rescue IL-1β and TNFα secretion by stimulated PdMo, suggesting that an intact phagocytic machinery of monocytes is required for the platelet-effect. Because platelet vesicles[38], or even platelet organelles[53], can be additionally internalized by endocytosis, we tested the inhibition of endocytosis on PdMos reconstituted with platelets[53]. However, the ability of platelets to rescue the faulty cytokine responses of PdMos was not impacted by the treatment of PdMo with Dynasore (DS), an inhibitor of dynamin 1/2 endocytosis[54] (**Figure 7H**).

Collectively, our findings support that platelets supply monocytes with functional p38 MAPK activity through the release of vesicles containing phosphorylated p38. These findings reveal an unprecedented mechanism of cell-to-cell communication and highlight a key role for platelets in licensing the pro-inflammatory cytokine responses of human monocytes.

DISCUSSION

Monocytes are highly plastic innate immune cells that coordinate numerous facets of host defense. They are also precursos of relevant immune cells such as macrophages and dendritic cells[55]. Monocytes have historically been defined by a combination of developmental origins, morphological and physical properties, expression of surface markers localization, and function. These criteria have defined the human monocyte pool into three subsets: classical ($CD14^{+}$ $CD16^{-}$), intermediate ($CD14^{+}$ $CD16^{+}$), and nonclassical ($CD14^{-}$ $CD16^{+}$) monocytes[1]. Current single-cell genomic technologies have facilitated the more comprehensive characterization of the phenotypic and functional states of human monocytes, including the identification of novel subpopulations[56]. However, this strategy for cell identification is inherently biased as it neglects information on the monocyte interactions with heterogeneous cells, including non-immune and tissue-resident cells, which are key determinants of monocyte functions[57-59]. For example, it has recently been demonstrated that interaction with platelets induces monocyte differentiation towards dendritic cells with enhanced cross-presentation capacity, and more efficiently activate $CD8_{+}$ T cells [24]. Here, we revealed an additional layer of immune regulation in blood circulating cells in which platelets are key to license the pro-inflammatory cytokine responses of classical human monocytes.

Monocytes form heterotypical interactions with platelets in steady state, which are increased during inflammation.

Formation of monocyte-platelet aggregates (MPAs) is a hallmark of monocyte-driven inflammation associated with different diseases[19, 20, 60], yet the pathological functions of MPAs have not been fully elucidated. It has been reported that the pro-inflammatory functions of monocytes are enhanced upon their interaction with platelets in numerous diseases[61-64]. Platelets influence the effector functions of monocytes, such as their extravasation through endothelial layers, increase their oxidative burst, and regulate the expression of various cytokines and chemokines. However, the molecular mechanisms by which platelets regulate monocyte functions are not fully elucidated[65]. Moreover, studies in the human system are lacking, and were mostly done in conditions where platelets are added to human monocytes, or describing pathological conditions where monocyte-platelet aggregation is enhanced. Using a platelet-depletion approach in human cells, and two commonly used monocyte isolation kits, we demonstrated that the cytokine output of primary human monocytes is directly proportional to the presence of platelets in cell preparations. Removal of platelets induced a state of immunoparalysis in human monocytes, characterized by a transcriptional shut-down of pro-inflammatory genes, and an impaired capacity to secrete cytokines in response to TLR and NLR activation.

Blood monocytes are also major systemic sources of pro-inflammatory mediators. While overactive $CD14^+$ monocytes mediate hyper-inflammation and cytokine storms, hypo-responsive (or dysfunctional) monocytes are continuously observed in association with immunoparalysis, a phenomenon observed in occasions of increased blood loss, such as trauma, major organ surgery[66], hemorrhagic fevers[67], sepsis[68, 69], liver failure[70, 71], and more recently in SARS-CoV-2 infections[12, 13]. Thrombocytopenia is a common feature among these different conditions. However, additional confounding factors, such as co-infections and lower leukocyte counts, render it difficult to assess the actual contribution of platelets to monocyte immunoparalysis. Our study identifies a similar state of hypo-responsiveness in monocytes isolated from conditions of low platelet counts, in the absence of infections or other known causes of thrombocytopenia. We demonstrated that the cytokine effector functions of blood monocytes from ITP patients are naturally impaired. Remarkably, we discovered that the immunoparalysis of platelet-depleted monocytes can be reversed by their supplementation with fresh autologous platelets. We further demonstrated the ability of healthy platelets to revert the immunoparalysis of ITP monocytes. These findings highlight platelets as essential co-factors determining the magnitude of monocyte innate immune programs, and may have consequences for the treatment of immunosuppression, or other life-threatening conditions associated with unchecked monocyte responses[6, 8].

Infections are associated with extensive platelet consumption and thrombocytopenia. Beside their roles in recruiting and facilitating the extravasation of leukocytes into the tissue[29, 72], platelets actively counteract infections by directly killing[73] or immobilizing pathogens[74, 75], thereby, facilitating their killing by neutrophils. All these processes result in platelet-consumption and loss of vascular integrity. In humans, thrombocytopenia is associated with increased mortality and disturbed immune defense programs during sepsis independently of disease severity[76]. In a randomized clinical trial, two anti-platelet medications reduced MPA formation and the systemic levels of CCL2, IL-6, IL-8, and TNFα in humans challenged with intravenous injection of *Escherichia coli* LPS [77]. However, depending on the disease setting, platelets attenuate monocyte inflammatory responses by triggering the production of IL-10 or sequestering IL-6 and TNF-α released by monocytes[30].

How platelet-monocyte interactions regulate monocyte functions remain largely unknown[65]. Our study reveals an unprecedented mechanism by which platelets regulate monocyte innate immunity and identifies platelet-derived p38 MAPK signaling as a critical trans-cellular regulator of cytokine production in monocytes. We demonstrated that the addition of fresh platelets bypassed pharmacological p38 inhibition in human monocytes in a concentration-dependent manner. These findings have important clinical relevance as MAPK p38 inhibitors have become relevant targets of cytokine-suppressive anti-inflammatory drugs[78-80].

We also confirmed previous findings that platelets have abundant stocks of phosphorylated RelA (p65)[37, 39, 81]. We found that monocytes co-cultured with platelets and platelets alone had robust p65 levels. These results suggest that platelets may be potential sources of these molecules in the blood. It has been previously demonstrated that interaction with platelets enhances the nuclear translocation of p65 within monocytes [48, 81, 82]. However, the possibility that a considerable portion of p65 arises from platelets was never raised. In our experimental settings, inhibition of IKKβ phosphorylation with BAY was toxic to primary human monocytes, precluding us from addressing whether p65 was transferred from platelets to monocytes. Moreover, mounting evidence indicates that p38 MAPK signaling is upstream of NFκB in human platelets, and inhibition of MAPK prevents IKKβ and p65

phosphorylation[83, 84]. Hence, it is possible that the SB203580, used in our experiments to inhibit p38, had additional effects on p65 phosphorylation.

Though we have not clearly visualized phagocytosis of platelets by monocytes by confocal microscopy, using phagocytosis inhibitors, trans-well cultures, and transfer of platelet supernatants, we ruled out the involvement of a humoral platelet-derived factor and found that vesicles restore cytokine activity in platelet-depleted monocytes. We also observed numerous platelets bound to monocytes, supporting previous observations that a large fraction of blood monocytes (up to 45%) are physiologically associated with platelets in steady-state conditions[16]. Furthermore, breaking MPAs via interfering with P-sel-PSGL-1 interactions did not prevent the platelet effect on monocytes. This association between monocytes and platelets may be part of a homeostatic mechanism to equip monocyte immune functions for when they are needed.

Although the phagocytosis of platelets by monocytes is a likely scenario, and supported by our assays, it is also possible that cellular contacts allow the shuttling of molecules from platelets to monocytes, as previously demonstrated with cellular receptors[85], bioactive lipids[86, 87] and intact organelles[53] that are transferred from platelets, or platelet vesicles, to leukocytes, with preserved activity in the cytosol of recipient cells. Although we ruled out the participation of numerous well-known ligand-receptor interactions in the platelet-monocyte crosstalk, the mechanisms by which platelets supply p38 signaling to monocytes remain unidentified.

Recently, independent studies have demonstrated that the inflammasome activation in blood $CD14^+$ monocytes[6, 8] and lung macrophages [88] is implicated in the systemic hyper-inflammation that contributes to the severity of SARS-CoV2 infection. Our study revealed a critical role of platelets for the inflammasome activity of human monocytes, raising the question whether platelets may help to fuel inflammasome hyper activity[89] driving COVID-19 pathology[6, 8]. Indeed, immunothrombosis and platelet activation are hallmarks of severe COVID-19.

Classical monocytes are also key cells involved in trained immunity[15] a biological process of epigenetic adaptations that have long-lasting and broad benefits to host defense but also potentially detrimental outcomes in chronic inflammatory diseases. However, no study has yet investigated if and how the interactions with platelets influence the development of trained immunity. Our findings also open possibilities for clinical interventions of platelet/monocyte interaction with blocking/enhancing nanobodies. If possible, these would open potential avenues to drug patients with monocyte-dependent increased inflammation or chronic disease.

FUNDING

This study was funded by the European Research Council (EC | H2020 | H2020 Priority Excellent Science | H2020 European Research Council (ERC) PLAT-IL-1, 714175). Bernardo S Franklin is further supported by the Germany's Excellence Strategy (EXC 2151 – 390873048) from the Deutsche Forschungsgemeinschaft (DFG, German Research Foundation).

ACKNOWLEDGMENTS

We thank Marco A Ataide, Florian I Schmidt, and Dagmar Wachten for scientific discussions and input and for proofreading the manuscript. We thank Cornelia Rohland and Maximilian Rothe for technical help, and organization and maintenance of mouse lines, respectively. We thank Dr. Savithri Rangarajan and Dr. Rik de Wijn (PamGene, Diagnostic Assay Services, 's-Hertogenbosch, The Netherlands) for performing the peptide quality control and bioinformatics analysis of the Protein Kinase Assay. We also acknowledge H James Stunden for the assistance with the NanoString experiments. We thank the Microscopy and Flow Cytometry Core Facility of the Medical Faculty at the University of Bonn for providing help, services, and devices funded by the Deutsche Forschungsgemeinschaft (DFG, German Research Foundation, project number 388158066, 216372545 and 388159768). Finally, we thank Andrea Schlichting and Leonie Verwohlt for administrative support.

AUTHOR CONTRIBUTIONS

Ibrahim Hawwari: Investigation; Formal analysis; Data curation; Visualization; Methodology; Writing—review and editing. **Nathalia Sofia Rosero Reyes:** Investigation; Technical Support. **Lino L Teichmann** and **Lisa Meffert**: ITP patient samples. **Agnieszka Demczuk:** Investigation. **Lucas S. Ribeiro:** Technical Support. **Damien Bertheloot:** Supervision; Investigation; Writing—review and editing. **Bernardo S Franklin:** Conceptualization; Funding acquisition; Project administration; Resources; Formal analysis; Supervision; Validation; Investigation; Visualization; Writing—original draft.

REFERENCES

1. Wong, K.L., et al., Gene expression profiling reveals the defining features of the classical, intermediate, and nonclassical human monocyte subsets. Blood, 2011. 118(5): p. e16-31.

2. Fajgenbaum, D.C. and C.H. June, Cytokine Storm. N Engl J Med, 2020. 383(23): p. 2255-2273.
3. Jafarzadeh, A., et al., Contribution of monocytes and macrophages to the local tissue inflammation and cytokine storm in COVID-19: Lessons from SARS and MERS, and potential therapeutic interventions. Life Sci, 2020. 257: p. 118102.
4. Schulte-Schrepping, J., et al., Severe COVID-19 Is Marked by a Dysregulated Myeloid Cell Compartment. Cell, 2020. 182(6): p. 1419-1440 e23.
5. Bonnet, B., et al., Severe COVID-19 is characterized by the co-occurrence of moderate cytokine inflammation and severe monocyte dysregulation. EBioMedicine, 2021. 73: p. 103622.
6. Ferreira, A.C., et al., SARS-CoV-2 engages inflammasome and pyroptosis in human primary monocytes. Cell Death Discovery, 2021. 7(1): p. 43.
7. Vanderbeke, L., et al., Monocyte-driven atypical cytokine storm and aberrant neutrophil activation as key mediators of COVID-19 disease severity. Nat Commun, 2021. 12(1): p. 4117.
8. Junqueira, C., et al., FcγR-mediated SARS-CoV-2 infection of monocytes activates inflammation. Nature, 2022.
9. Frazier, W.J. and M.W. Hall, Immunoparalysis and adverse outcomes from critical illness. Pediatr Clin North Am, 2008. 55(3): p. 647-68, xi.
10. Arens, C., et al., Sepsis-induced long-term immune paralysis--results of a descriptive, explorative study. Crit Care, 2016. 20: p. 93.
11. Roquilly, A., et al., Alveolar macrophages are epigenetically altered after inflammation, leading to long-term lung immunoparalysis. Nat Immunol, 2020. 21(6): p. 636-648.
12. Agrati, C., et al., Expansion of myeloid-derived suppressor cells in patients with severe coronavirus disease (COVID-19). Cell Death Differ, 2020. 27(11): p. 3196-3207.
13. Arunachalam, P.S., et al., Systems biological assessment of immunity to mild versus severe COVID-19 infection in humans. Science, 2020. 369(6508): p. 1210-1220.
14. Bekkering, S., et al., Oxidized low-density lipoprotein induces long-term proinflammatory cytokine production and foam cell formation via epigenetic reprogramming of monocytes. Arterioscler Thromb Vasc Biol, 2014. 34(8): p. 1731-8.
15. Netea, M.G., et al., Trained immunity: A program of innate immune memory in health and disease. Science, 2016. 352(6284): p. aaf1098.
16. Rinder, H.M., et al., Dynamics of leukocyte-platelet adhesion in whole blood. Blood, 1991. 78(7): p. 1730-7.
17. Stephen, J., et al., The uncoupling of monocyte-platelet interactions from the induction of proinflammatory signaling in monocytes. J Immunol, 2013. 191(11): p. 5677-83.
18. Liang, H., et al., Higher levels of circulating monocyte-platelet aggregates are correlated with viremia and increased sCD163 levels in HIV-1 infection. Cell Mol Immunol, 2015. 12(4): p. 435-43.
19. Allen, N., et al., Circulating monocyte-platelet aggregates are a robust marker of platelet activity in cardiovascular disease. Atherosclerosis, 2019. 282: p. 11-18.
20. Manne, B.K., et al., Platelet gene expression and function in patients with COVID-19. Blood, 2020. 136(11): p. 1317-1329.
21. Rodrigues, T.S., et al., Inflammasomes are activated in response to SARS-CoV-2 infection and are associated with COVID-19 severity in patients. J Exp Med, 2021. 218(3).
22. Rolfes, V., et al., Platelets Fuel the Inflammasome Activation of Innate Immune Cells. Cell Rep, 2020. 31(6): p. 107615.
23. Bhattacharjee, J., et al., Monocytes isolated by positive and negative magnetic sorting techniques show different molecular characteristics and immunophenotypic behaviour. F1000Res, 2017. 6: p. 2045.
24. Han, P., et al., Platelet P-selectin initiates cross-presentation and dendritic cell differentiation in blood monocytes. Sci Adv, 2020. 6(11): p. eaaz1580.
25. Ambayya, A., et al., Haematological reference intervals in a multiethnic population. PLoS One, 2014. 9(3): p. e91968.
26. Broz, P. and V.M. Dixit, Inflammasomes: mechanism of assembly, regulation and signalling. Nature Reviews Immunology, 2016. 16(7): p. 407-420.
27. Cooper, N. and W. Ghanima, Immune Thrombocytopenia. N Engl J Med, 2019. 381(10): p. 945-955.
28. Xiang, B., et al., Platelets protect from septic shock by inhibiting macrophage-dependent inflammation via the cyclooxygenase 1 signalling pathway. Nature Communications, 2013. 4: p. 264.
29. Sreeramkumar, V., et al., Neutrophils scan for activated platelets to initiate inflammation. Science (New York, NY), 2014. 346(6214): p. 1234-1238.
30. Carestia, A., et al., Platelets Promote Macrophage Polarization toward Pro-inflammatory Phenotype and Increase Survival of Septic Mice. CellReports, 2019. 28(4): p. 896-908.e5.
31. Alasoo, K., et al., Transcriptional profiling of macrophages derived from monocytes and iPS cells identifies a conserved response to LPS and novel alternative transcription. Sci Rep, 2015. 5: p. 12524.
32. Pachot, A., et al., Decreased expression of the fractalkine receptor CX3CR1 on circulating monocytes as new feature of sepsis-induced immunosuppression. J Immunol, 2008. 180(9): p. 6421-9.
33. Solt, L.A. and M.J. May, The IkappaB kinase complex: master regulator of NF-kappaB signaling. Immunol Res, 2008. 42(1-3): p. 3-18.
34. Vega-Sendino, M., et al., The ETS transcription factor ERF controls the exit from the naive pluripotent state in a MAPK-dependent manner. Sci Adv, 2021. 7(40): p. eabg8306.
35. Zhao, B., et al., Annexin A1 translocates to nucleus and promotes the expression of pro-inflammatory cytokines in a PKC-dependent manner after OGD/R. Scientific Reports, 2016. 6(1): p. 27028.
36. Ezumi, Y., H. Takayama, and M. Okuma, Thrombopoietin, c-Mpl ligand, induces tyrosine phosphorylation of Tyk2, JAK2, and STAT3, and enhances agonists-induced aggregation in platelets in vitro. FEBS Lett, 1995. 374(1): p. 48-52.
37. Beaulieu, L.M. and J.E. Freedman, NFkappaB regulation of platelet function: no nucleus, no genes, no problem? J Thromb Haemost, 2009. 7(8): p. 1329-32.
38. Lannan, K.L., et al., Breaking the mold: transcription factors in the anucleate platelet and platelet-derived microparticles. Front Immunol, 2015. 6: p. 48.
39. Poli, V., et al., Inhibition of transcription factor NFAT activity in activated platelets enhances their aggregation and exacerbates gram-negative bacterial septicemia. Immunity, 2021.
40. Saklatvala, J., et al., Role for p38 mitogen-activated protein kinase in platelet aggregation caused by collagen or a thromboxane analogue. J Biol Chem, 1996. 271(12): p. 6586-9.
41. Kasper, C.A., et al., Cell-Cell Propagation of NF-κB Transcription Factor and MAP Kinase Activation Amplifies Innate Immunity against Bacterial Infection. Immunity, 2010. 33(5): p. 804-816.
42. Ablasser, A., et al., Cell intrinsic immunity spreads to bystander cells via the intercellular transfer of cGAMP. Nature, 2013. 503(7477): p. 530-534.
43. Yamashita, Y., M. Hishinuma, and M. Shimada, Activation of PKA, p38 MAPK and ERK1/2 by gonadotropins in cumulus cells is critical for induction of EGF-like factor and TACE/ADAM17 gene expression during in vitro maturation of porcine COCs. J Ovarian Res, 2009. 2: p. 20.

44. Lee, J.C., et al., A protein kinase involved in the regulation of inflammatory cytokine biosynthesis. Nature, 1994. 372(6508): p. 739-746.
45. White, D.E. and S.A. Burchill, BAY 11-7082 induces cell death through NF-kappaB-independent mechanisms in the Ewing's sarcoma family of tumours. Cancer Lett, 2008. 268(2): p. 212-24.
46. Rauert-Wunderlich, H., et al., The IKK inhibitor Bay 11-7082 induces cell death independent from inhibition of activation of NFkappaB transcription factors. PLoS One, 2013. 8(3): p. e59292.
47. Frenette, P.S., et al., P-Selectin glycoprotein ligand 1 (PSGL-1) is expressed on platelets and can mediate platelet-endothelial interactions in vivo. J Exp Med, 2000. 191(8): p. 1413-22.
48. Weyrich, A.S., et al., Monocyte tethering by P-selectin regulates monocyte chemotactic protein-1 and tumor necrosis factor-alpha secretion. Signal integration and NF-kappa B translocation. Journal of Clinical Investigation, 1995. 95(5): p. 2297-2303.
49. Forlow, S.B., R.P. McEver, and M.U. Nollert, Leukocyte-leukocyte interactions mediated by platelet microparticles under flow. Blood, 2000. 95(4): p. 1317-23.
50. Lang, D., et al., Down-regulation of monocyte apoptosis by phagocytosis of platelets: involvement of a caspase-9, caspase-3, and heat shock protein 70-dependent pathway. J Immunol, 2002. 168(12): p. 6152-8.
51. Maugeri, N., et al., Neutrophils phagocytose activated platelets in vivo: a phosphatidylserine, P-selectin, and {beta}2 integrin-dependent cell clearance program. Blood, 2009. 113(21): p. 5254-65.
52. Senzel, L. and C. Chang, Platelet phagocytosis by neutrophils. Blood, 2013. 122(9): p. 1543.
53. Levoux, J., et al., Platelets Facilitate the Wound-Healing Capability of Mesenchymal Stem Cells by Mitochondrial Transfer and Metabolic Reprogramming. Cell Metab, 2021. 33(2): p. 283-299 e9.
54. Ma, T., et al., Low-dose metformin targets the lysosomal AMPK pathway through PEN2. Nature, 2022. 603(7899): p. 159-165.
55. Guilliams, M., A. Mildner, and S. Yona, Developmental and Functional Heterogeneity of Monocytes. Immunity, 2018. 49(4): p. 595-613.
56. Villani, A.C., et al., Single-cell RNA-seq reveals new types of human blood dendritic cells, monocytes, and progenitors. Science, 2017. 356(6335).
57. Naik, S., et al., Compartmentalized control of skin immunity by resident commensals. Science, 2012. 337(6098): p. 1115-9.
58. Brewitz, A., et al., CD8(+) T Cells Orchestrate pDC-XCR1(+) Dendritic Cell Spatial and Functional Cooperativity to Optimize Priming. Immunity, 2017. 46(2): p. 205-219.
59. Medaglia, C., et al., Spatial reconstruction of immune niches by combining photoactivatable reporters and scRNA-seq. Science, 2017. 358(6370): p. 1622-1626.
60. Barrett, T.J., et al., Platelet regulation of myeloid suppressor of cytokine signaling 3 accelerates atherosclerosis. Sci Transl Med, 2019. 11(517).
61. Rong, M.Y., et al., Platelets induce a proinflammatory phenotype in monocytes via the CD147 pathway in rheumatoid arthritis. Arthritis Res Ther, 2014. 16(6): p. 478.
62. D'Mello, C., et al., Interactions Between Platelets and Inflammatory Monocytes Affect Sickness Behavior in Mice With Liver Inflammation. Gastroenterology, 2017. 153(5): p. 1416-1428.e2.
63. Singhal, R., et al., Development of pro-inflammatory phenotype in monocytes after engulfing Hb-activated platelets in hemolytic disorders. Clinical Immunology, 2017. 175: p. 133-142.
64. Fu, G., et al., Platelet-Monocyte Aggregates: Understanding Mechanisms and Functions in Sepsis. Shock, 2021. 55(2): p. 156-166.
65. Kral, J.B., et al., Platelet Interaction with Innate Immune Cells. Transfus Med Hemother, 2016. 43(2): p. 78-88.
66. Haupt, W., et al., Monocyte function before and after surgical trauma. Dig Surg, 1998. 15(2): p. 102-4.
67. Vangeti, S., et al., Monocyte subset redistribution from blood to kidneys in patients with Puumala virus caused hemorrhagic fever with renal syndrome. PLoS Pathog, 2021. 17(3): p. e1009400.
68. Cao, C., M. Yu, and Y. Chai, Pathological alteration and therapeutic implications of sepsis-induced immune cell apoptosis. Cell Death Dis, 2019. 10(10): p. 782.
69. Weisheit, C.K., et al., Sustained Immunoparalysis in Endotoxin-Tolerized Monocytic Cells. Mediators Inflamm, 2020. 2020: p. 8294342.
70. Wasmuth, H.E., et al., Patients with acute on chronic liver failure display "sepsis-like" immune paralysis. J Hepatol, 2005. 42(2): p. 195-201.
71. Lin, C.Y., et al., Endotoxemia contributes to the immune paralysis in patients with cirrhosis. J Hepatol, 2007. 46(5): p. 816-26.
72. Zuchtriegel, G., et al., Platelets Guide Leukocytes to Their Sites of Extravasation. PLoS Biology, 2016. 14(5): p. e1002459.
73. McMorran, B.J., et al., Platelet factor 4 and Duffy antigen required for platelet killing of Plasmodium falciparum. Science, 2012. 338(6112): p. 1348-51.
74. Wong, C.H.Y., et al., Nucleation of platelets with blood-borne pathogens on Kupffer cells precedes other innate immunity and contributes to bacterial clearance. Nature Immunology, 2013. 14(8): p. 785-792.
75. Gaertner, F., et al., Migrating Platelets Are Mechano-scavengers that Collect and Bundle Bacteria. Cell, 2017. 171(6): p. 1368-1382.e23.
76. Claushuis, T.A.M., et al., Thrombocytopenia is associated with a dysregulated host response in critically ill sepsis patients. Blood, 2016. 127(24): p. 3062-3072.
77. Thomas, M.R., et al., Platelet P2Y12 Inhibitors Reduce Systemic Inflammation and Its Prothrombotic Effects in an Experimental Human Model. Arterioscler Thromb Vasc Biol, 2015. 35(12): p. 2562-70.
78. Yong, H.Y., M.S. Koh, and A. Moon, The p38 MAPK inhibitors for the treatment of inflammatory diseases and cancer. Expert Opin Investig Drugs, 2009. 18(12): p. 1893-905.
79. Anand, P., et al., Clinical trial of the p38 MAP kinase inhibitor dilmapimod in neuropathic pain following nerve injury. Eur J Pain, 2011. 15(10): p. 1040-8.
80. Christie, J.D., et al., A Randomized Dose-Escalation Study of the Safety and Anti-Inflammatory Activity of the p38 Mitogen-Activated Protein Kinase Inhibitor Dilmapimod in Severe Trauma Subjects at Risk for Acute Respiratory Distress Syndrome. Crit Care Med, 2015. 43(9): p. 1859-69.
81. Weyrich, A.S., et al., Activated platelets signal chemokine synthesis by human monocytes. Journal of Clinical Investigation, 1996. 97(6): p. 1525-1534.
82. Ueda, A., et al., NF-kappa B and Sp1 regulate transcription of the human monocyte chemoattractant protein-1 gene. J Immunol, 1994. 153(5): p. 2052-63.
83. Lu, W.J., et al., A novel role of andrographolide, an NF-kappa B inhibitor, on inhibition of platelet activation: the pivotal mechanisms of endothelial nitric oxide synthase/cyclic GMP. J Mol Med (Berl), 2011. 89(12): p. 1261-73.
84. Lu, W.J., et al., Suppression of NF-kappaB signaling by andrographolide with a novel mechanism in human platelets: regulatory roles of the p38 MAPK-hydroxyl radical-ERK2 cascade. Biochem Pharmacol, 2012. 84(7): p. 914-24.

85. Rozmyslowicz, T., et al., Platelet-and megakaryocyte-derived microparticles transfer CXCR4 receptor to CXCR4-null cells and make them susceptible to infection by X4-HIV. Aids, 2003. 17(1): p. 33-42.
86. Barry, O.P., et al., Transcellular activation of platelets and endothelial cells by bioactive lipids in platelet microparticles. J Clin Invest, 1997. 99(9): p. 2118-27.
87. Rossaint, J., et al., Directed transport of neutrophil-derived extracellular vesicles enables platelet-mediated innate immune response. Nature Communications, 2016. 7: p. 13464.
88. Sefik, E., et al., Inflammasome activation in infected macrophages drives COVID-19 pathology. Nature, 2022.
89. Pan, P., et al., SARS-CoV-2 N protein promotes NLRP3 inflammasome activation to induce hyperinflammation. Nature Communications, 2021. 12(1): p. 4664.
90. Alard, J.-E., et al., Recruitment of classical monocytes can be inhibited by disturbing heteromers of neutrophil HNP1 and platelet CCL5. Science translational medicine, 2015. 7(317): p. 317ra196-317ra196.

METHODS

Reagents

Cell culture reagents (e.g., PBS, Fetal calf serum, GlutaMax, and RPMI) were from Gibco, Thermo Fisher Scientific. Stimuli were as follow: LPS (Ultrapure from E.coli O111:B4), Pam4CysK4, and R848 (Resiquimod) were from Invivogen. Nigericin acid was from Thermo Fisher Scientific. Inhibitors used were Cytochalasin D, BAY 11-7082 (Sigma-Aldrich). The CellTiter-Blue™ Cell Viability Assay and Caspase-Glo. 1 Inflammasome Assay were from Promega. HTRF kits to detect IL-1b, IL-6, TNFa, and NFkB were from Cisbio. ProcartaPlex™ kits for the detection of other Cytokine/Chemokine/Growth Factors were from Invitrogen. Antibodies were as follow: anti-IL-1b antibody (BAF401, R&D Systems, 1:1,000). DRAQ5 was from Thermo Fisher Scientific. For FACS, we used FcR Blocking Reagent, human and mouse (Miltenyi Biotec). Anti-human CD41 directly conjugated to Alexa Fluor 488 (Clone: HIP8), Anti-human CD14-A647 (Clone: HCD14) and isotype Mouse IgG1, k Isotype Ctrl (Clone: MOPC-21) Antibody were all from BioLegend.

Study Subjects

Peripheral blood was obtained by venipuncture of healthy volunteers after signature of informed consent, and approval of the study by the Ethics Committee of the University of Bonn (Protocol #282/17), and in accordance with the Declaration of Helsinki. Patients with Immuno Thrombocytopenia were recruited from a tertiary hematology referral hospital. We recruited 5 patients (3 female and 2 males, average age of 46 ± 9) from December 2019 to may 2020. All patients were diagnosed with ITP and comorbidities/infections were rule out. Written informed consent was obtained from all subjects according to the Declaration of Helsinki and approval by the Institutional Review Board of the University of Bonn (313/21). All participants were instructed about the objectives of the study and signed an informed consent in accordance with guidelines for human research.

Table 1 - Demographic and clinical characteristics of ITP patients (n = 5)

Age (mean ± SD)	46 ± 9
Gender Female/Male	3/2
Confirmed ITP Diagnosis (%)	100 %
Duration since diagnosis - years mean ± SD	6.5 ± 5.9
Laboratory results at baseline	
Platelet counts - G/L mean ± SD (Reference Ranges: 150 - 370).	53 ± 26
Leukocyte count - G/L mean ± SD (Reference Ranges: 3.9 - 10.2)	6.8 ± 4.2
CRP - mg/L mean ± SD (Reference Ranges: 0 - 3)	1.9 ± 1.8

Primary cells:

Primary human monocytes were isolated from peripheral blood collected from healthy volunteers in S-Monovette K3EDTA tubes. Blood was diluted 1:3 in PBS, and peripheral blood mononuclear cells (PBMCs) isolated using Ficoll® Paque PLUS density gradient centrifugation at 700 x g, 20 min. Primary human CD14+ monocytes were isolated from PBMCs using positive magnetic separation with the Classical Monocyte Isolation Kit (Miltenyi Biotech), or negative selection with the EasySep™ Human Monocyte Isolation Kit (STEMCELL™ Technologies) following manufacturers instructions. Platelet-depleted monocytes were generated by adding a Platelet Removal Component (50 µl ml^{-1}) supplied with the isolation kit (STEMCELL™ Technologies). Purity of monocyte populations was assessed by flow cytometry. Cells were incubated with FcR Blocking Reagent for 15 min at 37 °C, followed by staining with fluorochrome-conjugated monoclonal antibodies against human CD14 APC (eBioscience), anti-CD45 PE (eBioscience), and anti-CD41a FITC (eBioscience) for 30 min at RT. Cells were washed with PBS and fluorescence measured on a MACSQuant® Analyzer 10.

Platelet isolation

Human platelets were isolated from venous blood from healthy volunteers collected as previously described[22, 90]. Briefly, whole blood was centrifuged at 330 x g for 15 min and platelet-rich plasma (PRP) was collected. To prevent platelet aggregation during isolation, PRP was treated with 200 nM Prostaglandin E1 (PGE1), diluted 1:1 with PBS and centrifuged at 240 x g for 10 min to pellet leukocytes.

Platelet suspensions were collected and washed by centrifugation at 430 xg for 15 min in the presence of PBS PGE1. Washed platelets were pellet and resuspended in pre-warmed RPMI. To assess the purity and activation of isolated cells, human platelets were stimulated with 1 U ml−1 Thrombin from human plasma (Sigma-Aldrich) or left unstimulated for 30 min. Platelets were incubated with FcR Blocking Reagent followed by staining with CD45 (leukocyte marker), and CD41a FITC (eBioscience) and anti-CD62P APC (eBioscience).

Generation of platelet supernatants

Platelet supernatants were generated from suspensions of 1 x 10^8 human platelets incubated in RPMI and left untreated (PltSups) or stimulated with 2 ng ml−1 LPS (PltsLPS-Sups) for 4.5 h at 37°C. Cell suspensions were centrifuged at 3,000 x g for 10 min, the platelet supernatants were harvested and used to stimulate human monocytes.

Cell lines

The human monocytic THP-1 cell line (ATCC TIB-202) and the THP-1 DualTM reporter cell (InvivoGen, Thpd-nfis) were culture in RPMI supplemented with 10% heat-inactivated fetal calf serum, 1% Penicillin/Streptomycin and 1x GlutaMax. For THP-1 DualTM cells, the growth medium contained additionally 25 mM HEPES. Cells were either studied in a monocyte-like phenotype (without PMA-differenciation) or after their differentiation into macrophages by PMA (50 µM) treatment for 24 h.

Stimulation Assays

Monocytes (1 x 10^5/well) were cultured alone or co-cultured with 50 (5 x 10^6/well), to 100 platelets (1 x 10^7/well). For stimulation, cells were treated with agonists of TLR1/2: Pam3CSK4 (1 µg ml^{-1}); TLR4: LPS (2 ng ml^{-1}); or TLR7/8: Resiquimod R848 (3.5 µg ml^{-1}); for for 4.5h. For inflammasome activation, cells were primed with a TLR agonist for 3 h (indicated in figures), followed by activation with nigericin (10 µM, 90 min) PrgI from *Bacillus anthracis* (100 ng ml^{-1}) and protective antigen (PA, 1 µg ml^{-1}), for 90 min) or transfection of poly(dA:dT, 0.5 µg ml^{-1}, 3 h). After stimulation, CFS were harvested and used for cytokine detection.

Cytokine measurement

Cytokine were detected in cell-free supernatants, or whole cell lysates by homogeneous time-resolved fluorescence technology (HTRF, Cisbio) according to the manufacturer instruction. A Human ProcartaPlexTM (Invitrogen) immunoassay was additinally used to to detect 45 human cytokines, chemokines and growth factor, according to the manufacturer instructions using a MAGPIX® System.

Cell Viability Assays

Cell viability was determined by measuring the release of Lactate Dehydrogenase Assay (LDH) in CFS, or the CellTiter-Blue Assay (CTB) in stimulated cells. For LDH measurement, CFS from stimulated cells were incubated with LDH buffer for 30 min at 37 °C without CO2, and absorbance was measured at 490 nm using a Spectramax i3 plate reader (ThermoFisher). Cells were incubated with CTB buffer at 37°C and the fluorescence read at different time points. In both assays, cells treated with Triton X-100 served as a 100% cell death control. Fluorescence was detected with a SpectraMax.

Assessment of Caspase-1 Activity

The specific activity of Caspase-1 was assessed in cell-free supernatants using Caspase-Glo® 1 Inflammasome Assay (Promega). Briefly, CFS were mixed 1:1 with Glo Buffer and incubated for 30 min at RT. Luminescence was measured with SpectraMax i3 (Molecular devices).

Trans-well assays

Human primary $CD14^+$ monocytes were seeded at a concentration of 1 x 10^5/well in HTS 0.4 mmTrans-well 96-well plates. Platelets were added to the upper wells at a concentration of 1 x 10^7 in RPMI. After addition of platelets, inflammasome activation was carried out as described above and the levels of cytokines were assessed in cell-free supernatants by HTRF and Luminex.

Confocal Imaging

Platelet interactions with human monocytes were imaged in a Leica TCS SP5 SMD confocal system (Leica Microsystem). Cells were seeded in microslide 8-Well IBIDI chamber, fixed with 4% paraformaldehyde (PFA) for 30 min, washed and incubated with staining mAbs in permeabilization/blocking buffer (10% goat serum, 1% FBS and 0.5% Triton X-100 in PBS) supplemented with human FcR Blocking Reagent for 30 min. Cells were stained overnight at 4°C with anti-human CD41Alexa Fluor 488; anti-human CD14-A647 or Hoechst 34580 (ThermoFisher).

Immunoblotting

Cells were lysed with RIPA complete lysis buffer supplemented with EDTA-free protease and phosphatase inhibitors (Roche), and 25 U of Benzonase Nuclease. Samples were loaded onto NuPAGETM Novex 4-12% Bis-

Tris gels, transfered to Immobilon-FL Polyvinylidene fluoride (PVDF) membranes. After blocking with 3% BSA [w/v] in Tris buffered saline (TBS), membranes were incubated overnight with primary antibodies diluted in TBS containing 3% BSA [w/v] and 0.1% Tween. After washing steps, membranes were incubated with secondary antibodies conjugated to IRDye680 or IRDye800 (1:25000) for 2 h at RT. Membrane was scanned at Odyssey Imager (Li-Cor Biosciences). The following primary antibodies were used for: β-Actin rabbit mAb (1:5000), Phospho-NF-kB p65 (Ser536) (93H1) Rabbit mAb #3033 (1:1000), NF-kB p65 (C22B4) Rabbit mAb #4764 (1:1000) and IkBa (L35A5) Mouse mAb (Amino-terminal Antigen) #4814 (1:1000).

Platelet depletion *in vivo*

In vivo platelet depletion was performed in female C57BL/6J mice (12 weeks) by intravenousl (i.v.) injection of 2 mg/kg of polyclonal rat anti-mouse GPIbα (R300) or same amounts of a polyclonal rat IgG none-immune (C301) antibody as control (Emfret Analytics). Mice were then challenged 12 hours later with i.v. injection of 2 mg/kg LPS, or PBS as control. Blood was collected after 3 h and PBMCs were isolated by density gradient centrifugation in Ficoll Paque PLUS. Mouse monocytes we isolated from PBMCs by FACS-sorting gating on Ly6G$^-$, IA/IE$^-$,CD45$^+$, CD11b$^+$, CD115$^+$ cells, and sorted directly into QIAzol lysis reagent. Lysates were frozen in liquid nitrogen and sent to GENEWIZ Azenta Life Sciences for bulk RNA sequencing. All animal experimentation were approved by the local ethical committee (LANUV-NRW #84-02.04.2016.A487). Mice were purchased from Charles River and housed at the House for Experimental Therapy (HET) of the University Hospital of Bonn.

Fluorescence-activated cell sorting was used to obtain mouse monocytes. Mouse blood monocytes were isolated from pooled blood of 4 mice per experimental groups, in 3 different experiments. For this, mouse PBMCs were isolated through Ficoll gradient and stained with anti-Ly6G BV785 (Biolegend, dillution: 1:40), anti-I-A/I-E BV785 (Biolegend, dillution: 1:80), anti CD45 FITC (Biolegend, dillution: 1:200), anti CD11b PE (eBioscience, dillution: 1:166), anti CD115 APC (Biolegend, dillution: 1:80) and Hoechst 33258 (Abcam, 1 µM) as viability staining. Finally, viable Ly6G-I-A/I-ECD45+ CD11b+CD115+ monocytes were sorted directly into QIAzol lysis reagent using the BD FACS Aria Fusion (387333827) and BD FACS Aria III (216372545) at the Flow Cytometry Core Facility of the Medical Faculty of the University of Bonn.

Bulk RNA sequencing of isolated murine monocytes

For bulk RNA sequencing, samples were processed according to the company's pipeline. RNA extraction was performed followed by a library preparation. Ultra-low input RNA-Seq was performed at Illumina HiSeq PE 2x150 bp with ~350M reads. Reads were then mapped to the Mus musculus GRCm38 reference genome (ENSEMBL) using the STAR aligner v.2.5.2b and unique gene hit counts were generated with the featureCounts from the Subread package v.1.5.2. Finally, standard analysis was performed by GENEWIZ. Differential gene expression analysis was performed using DESeq2, p-values and log2 fold changes were calculated by applying the Wald test and genes with adjusted p-value < 0.05 and absolute fold change > 2 were considered as significantly altered differentially expressed genes (DEGs). Data vizualization was created using the R package ggplot2.

Transcriptional Profiling of human monocytes and platelets with NanoString

The nCounter® Human Myeloid Innate Immunity Panel v2 (NanoString® Technologies) was used to assess the mRNA expression of 770 human transcripts, according to the manufacturer protocol. Briefly, single or co-cultures of monocytes and platelets were lysed in RLT Buffer (Qiagen) containing β-Meracptoethanol (1 x 10^4 cells/µl). RNA was isolated with and homogenized with CodeSets and left for hybridization overnight. RNA/CodeSet complexes were immobilized on nCounter cartridges at the nCounter® Prep Station 5s and data collection (RCC files) and quality check was performed in the nCounter® Digital Analyzer 5s. The nSolver™ Analysis and Partek® Genomics Suite® software was used for analysis.

Kinase activity profiling microarray. Primary monocytes, and platelets were isolated from 6 healthy donors. Monocytes were stimulated *ex vitro* before, or after the removal of platelets, or after re-adition of platelets to PdMo (biological replicates with n = 6). As before, platelets alone (n = 6) were assessed. Stimulated cultures were lysed in M-PER mammalian protein extraction reagent supplemented with PhosphoSTOP (Roche) and cOmplete Tablets (Roche), incubated on ice for 15 minutes. After centrifugation at 20.000x g for 15 minutes at 4 C the protein concentration in the supernatant is evaluated via Bradford assay. The lysate is aliquoted, snap frozen and stored at -80 C. Only unthawed aliquots are used for the kinase activity assay.

Ser/Thr Kinase (STK) activity profiling assays based on measuring peptide phosphorylation by protein kinases (PamGene International BV, The Netherlands) were performed as instructed by manufacturer. In summary, samples with 1 µg protein were applied on PamChip 4

arrays containing 144 (STK) or 196 (PTK) peptides immobilized on a porous aluminum oxide membrane. The peptide sequences (13 amino acids long) harbor phosphorylation sites and are correlated with one or multiple upstream kinases. Fluorescently labelled anti-phospho antibodies are used to detect phosphorylation activity of kinases present in the sample (8, 9). Instrument operation and imaging are controlled by the EVOLVE 2.0 software and quantified using BioNavigator 6.3 (BN6; PamGene International BV, The Netherlands). Signal intensities at multiple exposure times were integrated by linear regression (S100), Log2-transformed, and normalized using a Combat correction model for batch correction where the scaling parameters (mean / sd) are estimated using an empirical Bayes approach, which effectively reduces the noise associated with applying the correction (10, 11).

The normalized values were used to perform statistics comparing groups or the upstream kinase analysis (UKA) tool (BN6; PamGene international BV). The following statistical test is used to generate a list of differentially significant phosphorylated peptides: Paired T-test, for LPS effect/ comparisons; and ANOVA-PostHoc Test for multiple treatments versus Control for comparing each group to StdMo unstimulated in both unstimulated and LPS-15 min conditions. For Kinase interpretation (differential): In order to generate a ranked list of putative kinases responsible for differences in the peptide phosphorylation, PamGene's in-house method called Upstream Kinase Analysis (UKA) was used. For Pathway interpretation (differential): In order to generate a ranked list of possible canonical pathways (and networks) responsible for differences in the peptide phosphorylation, there are many open-source tools to perform this.

The phylogenetic kinome tree, useful to group the kinases into sequence families, is plotted using the online portal CORAL: http://phanstiel-lab.med.unc.edu/CORAL/ (12). The upstream kinase analysis functional scoring tool (PamGene International) rank-orders the top kinases differential between the two groups, the ranking factor being the final (median) kinase score (represented by node size). This score is based on a combined sensitivity score (difference between treatment and control groups, represented as node color) and specificity score for a set of peptides to kinase relationship that are derived from existing databases. An arbitrary threshold of a final score of 1.2 was applied, based on the specificity scores. Significant peptides (t-tests, p-value < 0.05) or kinases (UKA, final scores > 1.2) were imported to the MetaCore pathway analysis tool (Clarivate Analytics) where an enrichment analysis was performed for pathways and networks. It consists of matching the kinases or substrates in the kinome arrays data with functional ontologies in MetaCore. The probability of a random intersection between a set of IDs in the target list with ontology entities is estimated in p value of hypergeometric intersection. The lower p value means higher relevance of the entity to the dataset, which shows in higher rating for the entity. Direct interaction network algorithms were used to build interconnected networks within each comparison. The "Add interactions" feature was used to add the interaction between RIPK1 and the data present in the MetaCore™ database after it was built.

Statistical Analysis

Statistical analyses were performed with GraphPad Prism Version 9.0f. Unless indicated otherwise, all graphs are built from pooled data from a minimum of two independent experiments (biological replicates), performed in triplicates (technical replicates). All statistical analysis were preceded by normality and lognormality tests, followed by the recommended parametric or nonparametric tests. For most experiments with several groups (StdMo, PdMo, PdMo + Ptls and Plts, stimulated vs. unstimulated) P values were determined by two-way ANOVA with Tukey's or Sidak's or multiple comparison tests. No outliers were detected or removed from analysis. Additional statistical details are given in the respective figure legends, when appropriate.

Data Presentation

Unless indicated otherwise (in Figure legends), all graphs are represented as Floating Bars (with mean, and minimum to maximum values) and are built from pooled data from a minimum of two independent experiments (biological replicates), performed in triplicates (technical replicates) with monocytes or platelets from different donors. Each symbol represents the average from 3 technical replicates per donor, or experiment in the case of cell lines. Symbols are coded (●, ▼ , ■ , ●, etc.) to indicate donors so readers can track the internal variability between different donors, or experiments. Dots are semi-transparent, with darker symbols indicating overlapping points.